

Discontinuous Galerkin Method with Staggered Hybridization for a Class of Nonlinear Stokes Equations

Jie Du¹ · Eric T. Chung² · Ming Fai Lam² ·
Xiao-Ping Wang³

Received: 19 October 2017 / Revised: 9 February 2018 / Accepted: 14 February 2018 /
Published online: 9 March 2018
© Springer Science+Business Media, LLC, part of Springer Nature 2018

Abstract In this paper, we present a discontinuous Galerkin method with staggered hybridization to discretize a class of nonlinear Stokes equations in two dimensions. The utilization of staggered hybridization is new and this approach combines the features of traditional hybridization method and staggered discontinuous Galerkin method. The main idea of our method is to use hybrid variables to impose the staggered continuity conditions instead of enforcing them in the approximation space. Therefore, our method enjoys some distinctive advantages, including mass conservation, optimal convergence and preservation of symmetry of the stress tensor. We will also show that, one can obtain superconvergent and strongly divergence-free velocity by applying a local postprocessing technique on the approximate solution. We will analyze the stability and derive a priori error estimates of the proposed scheme. The resulting nonlinear system is solved by using the Newton's method, and some numerical results will be demonstrated to confirm the theoretical rates of convergence and superconvergence.

Keywords Discontinuous Galerkin method · Staggered hybridization · Nonlinear Stokes equations · Symmetric stress tensor

✉ Jie Du
jdu@mail.tsinghua.edu.cn

Eric T. Chung
tschung@math.cuhk.edu.hk

Ming Fai Lam
mflam@math.cuhk.edu.hk

Xiao-Ping Wang
mawang@ust.hk

¹ Yau Mathematical Sciences Center, Tsinghua University, Beijing, China

² Department of Mathematics, The Chinese University of Hong Kong, Sha Tin, Hong Kong SAR

³ Department of Mathematics, The Hong Kong University of Science and Technology, Clear Water Bay, Hong Kong SAR

1 Introduction

This paper is devoted to the design and analysis of a new discontinuous Galerkin (DG) method based on a staggered hybridization technique for a class of nonlinear Stokes problems. We will present our ideas in the two-dimensional case for the simplicity of presentation, but our method can be applied to the three-dimensional case. Let Ω be a bounded and simply connected domain in \mathbb{R}^2 with polygonal boundary $\partial\Omega$, where $\partial\Omega = \partial\Omega_D \cup \partial\Omega_N$ such that $\partial\Omega_D \neq \emptyset$ and $\partial\Omega_D \cap \partial\Omega_N = \emptyset$. We denote $\mathbf{u}(\mathbf{x}) = (u_1(\mathbf{x}), u_2(\mathbf{x}))^T$ as the velocity and μ as the viscosity of a given fluid. In general, $\mu = \mu(\mathbf{x}, \mathbf{u}(\mathbf{x}), \nabla\mathbf{u}(\mathbf{x})) \geq \mu_0 > 0$ is a positive scalar function, where μ_0 is a positive constant. Given a source term $\mathbf{f}(\mathbf{x}) \in [L^2(\Omega)]^2$ and boundary data $\mathbf{g}_D(\mathbf{x}) \in [H^{1/2}(\partial\Omega_D)]^2$ and $\mathbf{g}_N(\mathbf{x}) \in [H^{-\frac{1}{2}}(\partial\Omega_N)]^2$, we study the following nonlinear Stokes system problem:

$$\begin{aligned}
 -\operatorname{div}(\mu \varepsilon(\mathbf{u}) - p\mathbf{I}_2) &= \mathbf{f} && \text{in } \Omega, \\
 \operatorname{div} \mathbf{u} &= 0 && \text{in } \Omega, \\
 \mathbf{u} &= \mathbf{g}_D && \text{on } \partial\Omega_D, \\
 (\mu \varepsilon(\mathbf{u}) - p\mathbf{I}_2)\mathbf{n} &= \mathbf{g}_N && \text{on } \partial\Omega_N,
 \end{aligned}
 \tag{1}$$

where $\varepsilon(\mathbf{u}(\mathbf{x})) = \frac{\nabla\mathbf{u}(\mathbf{x}) + \nabla\mathbf{u}(\mathbf{x})^T}{2}$ is the strain tensor, $p(\mathbf{x})$ is the pressure, \mathbf{n} is the outward unit normal vector on $\partial\Omega$, \mathbf{I}_2 is the identity matrix and div denotes the row-wise divergence. To ensure the existence of a unique solution, we assume that the zero average condition for the pressure $\int_{\Omega} p \, dx = 0$ and the boundary data \mathbf{g}_D and \mathbf{g}_N satisfy the following compatibility conditions (see [2] for details):

$$\int_{\partial\Omega_D} \mathbf{g}_D \cdot \mathbf{n} \, ds = 0 \quad \text{and} \quad \int_{\Omega} \mathbf{f} \, dx + \int_{\partial\Omega_N} \mathbf{g}_N \, ds = 0.$$

In this paper, we assume that $\mu = \mu(\mathbf{x}, \varepsilon(\mathbf{u}))$ is a variable function depends on the strain tensor $\varepsilon(\mathbf{u})$.

For solving fluid flow problems, many variants of discontinuous Galerkin (DG) methods with different features have been developed [15, 17, 18, 25, 27, 30]. Among them, the staggered discontinuous Galerkin (SDG) method is developed for the Stokes equations in [21] and the Navier–Stokes equations in [5, 11] which combines some good properties of finite element methods and standard DG methods through the use of staggered grid. This edge-based (face-based in 3D) staggered grid used in the SDG method is different from the vertex based dual grid used in finite difference method (see [1]), as staggered continuities are given to the approximate variables when the edge-based staggered grid is used. In particular, normal component of velocity is continuous on a subset of edges and the pressure is continuous on the rest of the edges. This staggered continuity property naturally gives the interelement flux terms, so it is distinctive that, when compared to most of the other DG methods, no numerical flux or penalty parameter is needed. Besides the above advantages, the SDG method enjoys an optimal order of convergence and, for a variety of applications, some other nice properties including local and global conservation, energy conservation, low dispersion error, mass conservation and suitability for adaptive refinement (see [7–9, 21] for more details). Moreover, a relationship between the SDG method and the hybridizable discontinuous Galerkin (HDG) method has been shown in [6]. From this point of view, the SDG method shares some good properties with the HDG method, namely, the postprocessing and superconvergence.

Recently, a superconvergence HDG method is developed with the idea of M-decomposition [14].

Since many types of fluid are isotropic, such as ordinary gases and liquids, they lead to the symmetry of the stress tensor. However, the SDG formulation hinders the preservation of this symmetry, in particular, as the staggered continuities are defined in the finite element spaces, so it is not easy to construct symmetric finite element basis functions for the stress tensor. Therefore, we will develop a new DG method, which can retain the distinctive advantages of the SDG method and preserve the properties of the nonlinear Stokes equations (1), especially the symmetry of the stress tensor. These can be achieved by a technique of staggered hybridization, which uses some hybrid variables to enforce the staggered continuities on a staggered mesh.

Next, we discuss two distinctive features of our proposed method. First of all, we consider the second equation in (1), which is often referred as the incompressibility condition. In other words, it is an equation describing the conservation of mass. We emphasize that upon the use of staggered continuities, the resulting discrete system can preserve the structures of the continuous problem and the conservation of mass property (see [21] for details). Furthermore, the postprocessing technique in [6] can be used and shows that the postprocessed velocity is exactly divergence free. Secondly, we consider the first equation of (1), and we see that the stress tensor is symmetric. So, extra symmetry condition is needed to be imposed on the system. One may choose to use a weak symmetric approach, but then the preservation of the symmetry of the stress tensor is also weakened. Therefore, in order to enhance the accuracy of numerical solution, we will propose a DG method that can give an exactly symmetric approximation for the stress tensor and retain the nice properties of the SDG method by means of hybridization, which has been successfully applied in many DG methods (for example, [6, 16, 26]). By using such approach, the construction of basis functions are completely local, and the continuity of solution is enforced by means of hybridization. Besides the symmetry of the stress tensor, the idea for preserving the nonlinearity comes from the viscosity coefficient μ can also be inherited from [10], which considers solving the nonlinear elliptic problems with varying coefficient functions.

We remark here that the major differences between the SDG method and the new proposed DG method are the strongly enforced symmetry of the stress tensor in the finite element space, and the staggered continuity conditions are now relaxed in the finite element spaces, so hybrid variables will be used to retain the staggered continuities. Besides the use of hybridization, there are many other successful examples for solving the varying viscosity problems. For example, in [19], the focus is put onto the construction of preconditioner for the discrete system of equations. Moreover, an emphasis is placed on the situation when both the viscosity and the density are considered as variable functions for the incompressible Navier–Stokes equations in [23]. Furthermore, we remark that the model (1) can be applied to many physical problems, for example, the ice sheet dynamics [20], mantle convection [29] and fluid dynamics involving non-Newtonian fluids [13], which motivate the study in this paper.

The organization of the paper is as follows. In Sect. 2, we present the discrete formulation of our model with a detailed explanation of the staggered mesh, and the solution algorithm is also included. As our proposed method inherits several staggered properties from the SDG method, so after the presentation of the numerical scheme, some SDG related analytical results will be stated in Sect. 3. These results are important and can be seen as the preliminaries of the stability and convergence analysis of the proposed scheme in Sect. 4. Numerical examples will be illustrated in Sect. 5 to demonstrate the convergence order and accuracy of the method. Finally, in Sect. 6, we conclude the paper.

2 Numerical Scheme

In this section, we will construct a DG method with staggered hybridization so that we can achieve staggered continuity for the numerical solution. At the same time, we can preserve the symmetry of the numerical stress and obtain the nice properties of the SDG method.

2.1 Weak Formulation

To simplify the notation, we write $\mu(\varepsilon(\mathbf{u}))$ to represent $\mu(\mathbf{x}, \varepsilon(\mathbf{u}))$ in the remaining sections. Then, we introduce some auxiliary variables:

$$\begin{aligned} S &= \varepsilon(\mathbf{u}), \\ S^\mu &= \mu(\varepsilon(\mathbf{u})) \varepsilon(\mathbf{u}), \end{aligned}$$

so the problem (1) can be rewritten as:

$$S = \varepsilon(\mathbf{u}) \quad \text{in } \Omega, \tag{2a}$$

$$S^\mu = \mu(S)S \quad \text{in } \Omega, \tag{2b}$$

$$-\operatorname{div} S^\mu + \nabla p = \mathbf{f} \quad \text{in } \Omega, \tag{2c}$$

$$\operatorname{div} \mathbf{u} = 0 \quad \text{in } \Omega, \tag{2d}$$

$$\mathbf{u} = \mathbf{g}_D \quad \text{on } \partial\Omega_D, \tag{2e}$$

$$\boldsymbol{\sigma} \mathbf{n} = \mathbf{g}_N \quad \text{on } \partial\Omega_N, \tag{2f}$$

where $\boldsymbol{\sigma} = \mu(\varepsilon(\mathbf{u})) \varepsilon(\mathbf{u}) - p\mathbf{I}_2$ and the zero average condition for the pressure $\int_\Omega p \, dx = 0$ is imposed. In the above system, we can see that the symmetry of the strain tensor and the stress tensor is highly emphasized, so we need to construct a stable numerical scheme which can preserve this symmetry. Since many discontinuous Galerkin (DG) methods only give weakly symmetric numerical stress tensor when the variational formulation with weakly symmetric constraint is considered, so here we consider a variational formulation with the strong symmetry approach. We further introduce

$$\begin{aligned} \mathcal{W} &= [L^2(\Omega)]_{sym}^{2 \times 2}, \\ \mathcal{U} &= [H^1(\Omega)]^2, \\ \mathcal{P} &= L^2(\Omega), \end{aligned}$$

where $[L^2(\Omega)]_{sym}^{2 \times 2}$ denotes a subspace of $[L^2(\Omega)]^{2 \times 2}$, consisting of symmetric matrices only. Then, the variational form corresponding to system (2) is to find $(\mathbf{u}, S, S^\mu, p) \in \mathcal{U} \times \mathcal{W} \times \mathcal{W} \times \mathcal{P}$ such that

$$\begin{aligned} (S, \phi)_{0,\Omega} - (\varepsilon(\mathbf{u}), \phi)_{0,\Omega} &= 0 & \forall \phi \in \mathcal{W}, \\ (S^\mu, \psi)_{0,\Omega} - (\mu(S)S, \psi)_{0,\Omega} &= 0 & \forall \psi \in \mathcal{W}, \\ (-\operatorname{div} S^\mu, \mathbf{v})_{0,\Omega} + (\nabla p, \mathbf{v})_{0,\Omega} &= (\mathbf{f}, \mathbf{v})_{0,\Omega} & \forall \mathbf{v} \in \mathcal{U}, \\ (\operatorname{div} \mathbf{u}, q)_{0,\Omega} &= 0 & \forall q \in \mathcal{P}, \end{aligned}$$

where $(\cdot, \cdot)_{0,\Omega}$ denotes the usual $L^2(\Omega)$ inner product, the pressure p satisfies the zero average condition and the boundary conditions are assumed.

For the analysis of stability and optimal order of convergence of our numerical scheme with respect to the L^2 -norm, we follow [4] and state two important assumptions on the continuous problem (1) as follows: we define a mapping $A_\mu : [L^2(\Omega)]^{2 \times 2} \rightarrow [L^2(\Omega)]^{2 \times 2}$

by $A_\mu(\phi) = \mu(\phi)\phi \quad \forall \phi \in [L^2(\Omega)]^{2 \times 2}$, and assume that this mapping A_μ satisfies two additional conditions. The first condition is the strongly monotone condition, which can be stated as follows:

$$\int_\Omega \left(A_\mu(\phi) - A_\mu(\psi) \right) : (\phi - \psi) \, dx \geq C_M \int_\Omega |\phi - \psi|^2 \, dx, \tag{3}$$

for any $\phi, \psi \in [L^2(\Omega)]^{2 \times 2}$. Here, C_M is a positive constant independent of the mesh size h . Besides the strongly monotone condition, A_μ is also assumed to be Lipschitz continuous. In other words, there exists a positive constant C_L , independent of the mesh size h , such that

$$\|A_\mu(\phi) - A_\mu(\psi)\|_{0,\Omega} \leq C_L \|\phi - \psi\|_{0,\Omega}. \tag{4}$$

The strongly monotone and Lipschitz continuity conditions of the mapping A_μ are essential for the unique solvability of the continuous problem (1) (see [12] and [24] for more general theory).

2.2 Staggered Mesh

We follow [9] to define the triangulation as follows. The domain Ω is first triangulated into an initial shape regular triangulation \mathcal{T}_u , and we assume there is no hanging nodes in \mathcal{T}_u . \mathcal{F}_u and \mathcal{F}_u^0 are defined as the sets of all edges and interior edges of \mathcal{T}_u , respectively. We introduce the notation $\mathcal{S}(v)$ to denote the element in \mathcal{T}_u with v as its centroid. The element $\mathcal{S}(v)$ is then further divided into three subtriangles by connecting v to its vertices. The final triangulation and the set of new edges formed after this process are denoted as \mathcal{T} and \mathcal{F}_p , respectively.

To clarify the notation with respect to the edges, we define $\mathcal{F} = \mathcal{F}_u \cup \mathcal{F}_p$ to be the set of all edges in \mathcal{T} and $\mathcal{F}_0 = \mathcal{F}_u^0 \cup \mathcal{F}_p$ to be the set of all interior edges in \mathcal{T} . Moreover, we introduce the notation $\mathcal{F}_u^D = \mathcal{F}_u^0 \cup \partial\Omega_D$ and $\mathcal{F}_p^N = \mathcal{F}_p \cup \partial\Omega_N$, which will be used in our discrete formulation. An illustration of the final triangulation \mathcal{T} for a square domain and element $\mathcal{S}(v)$ can be found in Fig. 1.

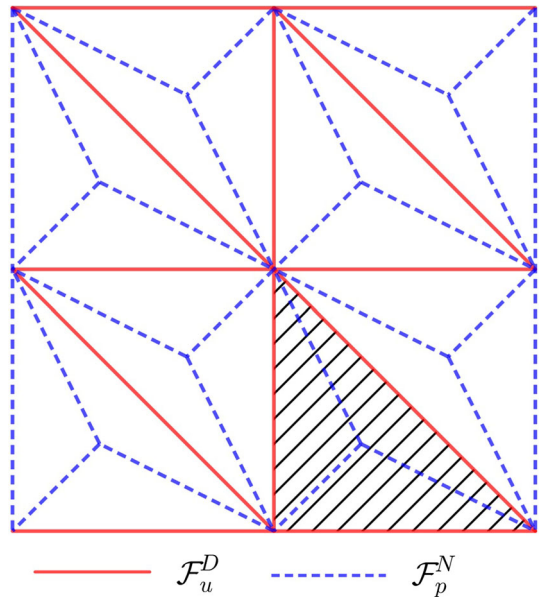
The main feature of the SDG method is the continuities of the finite element solutions \mathbf{u}_h and $\sigma_h \mathbf{n}$ over the edges \mathcal{F}_u^D and \mathcal{F}_p^N , respectively. However, in our method introduced in this paper, we relax this condition in the finite element spaces and we are ready to state the definitions of the corresponding finite element spaces that will be used in the discrete formulation of our method. Let k be a non-negative integer and $\tau \in \mathcal{T}$ be an element, the notation $P^k(\tau)$ and $P^k(e)$ are used to denote the space of polynomials with degree at most k on some element τ and edge e , respectively. Then the finite element spaces for velocity, gradient and pressure are defined in the order as

$$\begin{aligned} \mathcal{U}^h &= \{v : v|_\tau \in P^k(\tau), \forall \tau \in \mathcal{T}\}, \\ \mathcal{W}^h &= \{\phi : \phi|_\tau \in [P^k(\tau)]^{2 \times 2}, \forall \tau \in \mathcal{T}, \phi = \phi^T\}, \\ \mathcal{P}^h &= \{q : q|_\tau \in P^k(\tau), \forall \tau \in \mathcal{T}\}. \end{aligned}$$

From the definition of the finite element space for gradient, \mathcal{W}^h , we can see that every numerical variable $\phi_h \in \mathcal{W}^h$ is always strong symmetric.

Before we define the finite element spaces for the hybrid variables, we first define some jump operators over an edge e . For an element $\tau \in \mathcal{T}$, we define \mathbf{n}_τ as the outward unit normal vector on $\partial\tau$. And this notation will be simplified to \mathbf{n} if there is no confusion. For an interior edge $e \in \mathcal{F}_0$, there are two elements $\tau^+, \tau^- \in \mathcal{T}$ sharing this edge e . \mathbf{n}^+ and \mathbf{n}^- are denoted as the unit normal vectors pointing from τ^+ to τ^- and pointing from τ^- to τ^+ , respectively. For this interior edge e , we fix \mathbf{n}_e as one of \mathbf{n}^+ and \mathbf{n}^- . For a boundary

Fig. 1 An illustration of the triangulation \mathcal{T} on a square domain, where the red solid edges belong to \mathcal{F}_u^D and the blue dashed edges belong to \mathcal{F}_p^N . The shaded area in the bottom right corner represents the element $\mathcal{S}(v)$. Note that both $\partial\Omega_D$ and $\partial\Omega_N$ are non-empty (Color figure online)



edge $e \in \mathcal{F} \setminus \mathcal{F}_0$, the unit normal vector \mathbf{n}_e is defined as pointing outside Ω . Then the jump operator $[\mathbf{v}]|_e$ for a vector-valued function \mathbf{v} over an edge e is defined as

$$[\mathbf{v}]|_e = (\mathbf{n}^+ \cdot \mathbf{n}_e)\mathbf{v}^+ + (\mathbf{n}^- \cdot \mathbf{n}_e)\mathbf{v}^-,$$

where \mathbf{v}^+ and \mathbf{v}^- are the values of \mathbf{v} on e taking from τ^+ and τ^- , respectively. For a matrix-valued function ϕ , the corresponding jump operator $[\phi\mathbf{n}]|_e$ over an edge e is defined as

$$[\phi\mathbf{n}]|_e = \phi^+\mathbf{n}^+ + \phi^-\mathbf{n}^-,$$

where the meaning of ϕ^+ and ϕ^- are similar to \mathbf{v}^+ and \mathbf{v}^- .

Then, the finite element spaces for the hybrid variables are defined as

$$\mathcal{M}_u^h = \{\widehat{\phi} : \widehat{\phi}|_e \in P^k(e), \forall e \in \mathcal{F}_u^D\},$$

$$\mathcal{M}_p^h = \{\widehat{v} : \widehat{v}|_e \in P^k(e), \forall e \in \mathcal{F}_p^N\}.$$

The idea of our DG method is similar to the SDG method. However, instead of imposing staggered continuity of the approximate variables in the definition of finite element spaces, we now relax these constraints in the finite element space, and approximate \mathbf{u} , S , S^μ and p with $\mathbf{u}_h \in [\mathcal{U}^h]^2$, $S_h \in \mathcal{W}^h$, $S_h^\mu \in \mathcal{W}^h$ and $p_h \in \mathcal{P}^h$, respectively. Meanwhile, the approximation of the velocity $\mathbf{u}_h|_{\mathcal{F}_p^N}$ and the stress tensor $\sigma_h\mathbf{n}_e|_{\mathcal{F}_u^D} = (S_h^\mu - p_h\mathbf{I}_2)\mathbf{n}_e|_{\mathcal{F}_u^D}$ are shifted to the hybrid variables as $\widehat{\mathbf{u}}_h \in [\mathcal{M}_p^h]^2$ and $\widehat{\sigma}_h \in [\mathcal{M}_u^h]^2$, respectively. The continuities of \mathbf{u}_h on \mathcal{F}_u^D and $\sigma_h\mathbf{n}_e$ on \mathcal{F}_p^N are imposed as the following extra continuity conditions:

$$\int_e [\mathbf{u}_h] \cdot \widehat{\phi}_h \, ds = 0, \quad \forall \widehat{\phi}_h \in [\mathcal{M}_u^h]^2, \quad \forall e \in \mathcal{F}_u^D, \tag{5}$$

$$\int_e [\sigma_h\mathbf{n}] \cdot \widehat{v}_h \, ds = 0, \quad \forall \widehat{v}_h \in [\mathcal{M}_p^h], \quad \forall e \in \mathcal{F}_p^N. \tag{6}$$

On the boundary edge $e \in \partial\Omega_D$, the value of \mathbf{u}_h taken from the outside of Ω is considered as \mathbf{g}_D . Similarly, \mathbf{g}_N is considered as the value of $\sigma_h \mathbf{n} = (S_h^\mu - p_h \mathbf{I}_2) \mathbf{n}$ taken from the outside of Ω on boundary edge $e \in \partial\Omega_N$. Therefore, when e is a boundary edge, the above continuity conditions become the L^2 projections of the given boundary values.

2.3 Discrete System

We can then derive discrete formulation of a hybridized DG method with staggered continuity based on system (2). First, we multiply the Eq. (2a) by test function $\phi_h \in \mathcal{W}^h$, and integrating over $\tau \in \mathcal{T}$. Using integration by parts, we have

$$\int_\tau S : \phi_h \, dx + \int_\tau \mathbf{u} \cdot \operatorname{div}(\phi_h) \, dx - \int_{\partial\tau} \mathbf{u} \cdot (\phi_h \mathbf{n}) \, ds = 0. \tag{7}$$

Next, a test function $\psi_h \in \mathcal{W}^h$ is multiplied on both sides of Eq. (2b) and integrate over $\tau \in \mathcal{T}$, we obtain

$$\int_\tau S^\mu : \psi_h \, dx - \int_\tau \mu(S) S : \psi_h \, dx = 0. \tag{8}$$

Similarly, for the Eq. (2c), we multiply a test function $\mathbf{v}_h \in [\mathcal{U}^h]^2$ and integrate over each $\tau \in \mathcal{T}$. Integration by parts yields

$$\int_\tau S^\mu : \nabla \mathbf{v}_h \, dx - \int_{\partial\tau} (S^\mu \mathbf{n}) \cdot \mathbf{v}_h \, ds - \int_\tau p \operatorname{div}(\mathbf{v}_h) \, dx + \int_{\partial\tau} (p \mathbf{n}) \cdot \mathbf{v}_h \, ds = \int_\tau \mathbf{f} \cdot \mathbf{v}_h \, dx. \tag{9}$$

Finally, we multiply a test function $q_h \in \mathcal{P}^h$ on both sides of Eq. (2d) and integrate over $\tau \in \mathcal{T}$,

$$- \int_\tau \mathbf{u} \cdot \nabla q_h \, dx + \int_{\partial\tau} \mathbf{u} \cdot (q_h \mathbf{n}) \, ds = 0. \tag{10}$$

Then we replace \mathbf{u} , S , S^μ and p by the approximate solutions in the above weak formulation, we have

$$\int_\tau S_h : \phi_h \, dx + \int_\tau \mathbf{u}_h \cdot \operatorname{div}(\phi_h) \, dx - \int_{\partial\tau \cap \mathcal{F}_u^D} \mathbf{u}_h \cdot (\phi_h \mathbf{n}) \, ds - \int_{\partial\tau \cap \mathcal{F}_p^N} \widehat{\mathbf{u}}_h \cdot (\phi_h \mathbf{n}) \, ds = 0, \tag{11a}$$

$$\int_\tau S_h^\mu : \psi_h \, dx - \int_\tau \mu(S_h) S_h : \psi_h \, dx = 0, \tag{11b}$$

$$\begin{aligned} & \int_\tau S_h^\mu : \nabla \mathbf{v}_h \, dx - \int_{\partial\tau \cap \mathcal{F}_p^N} (S_h^\mu \mathbf{n}) \cdot \mathbf{v}_h \, ds - \int_\tau p_h \operatorname{div}(\mathbf{v}_h) \, dx \\ & + \int_{\partial\tau \cap \mathcal{F}_p^N} (p_h \mathbf{n}) \cdot \mathbf{v}_h \, ds - \int_{\partial\tau \cap \mathcal{F}_u^D} (\mathbf{n} \cdot \mathbf{n}_e) \widehat{\sigma}_h \cdot \mathbf{v}_h \, ds = \int_\tau \mathbf{f} \cdot \mathbf{v}_h \, dx, \end{aligned} \tag{11c}$$

$$- \int_\tau \mathbf{u}_h \cdot \nabla q_h \, dx + \int_{\partial\tau \cap \mathcal{F}_u^D} \mathbf{u}_h \cdot (q_h \mathbf{n}) \, ds + \int_{\partial\tau \cap \mathcal{F}_p^N} \widehat{\mathbf{u}}_h \cdot (q_h \mathbf{n}) \, ds = 0, \tag{11d}$$

for any $\tau \in \mathcal{T}$, and test functions $(\phi_h, \psi_h, \mathbf{v}_h, q_h) \in \mathcal{W}^h \times \mathcal{W}^h \times [\mathcal{U}^h]^2 \times \mathcal{P}^h$.

Then summing all the equations of system (11) over all elements $\tau \in \mathcal{T}$, with the extra staggered continuity conditions (5) and (6), the desired discrete formulation for (2) can be

rewritten as: find $(\mathbf{u}_h, S_h, S_h^\mu, p_h, \widehat{\mathbf{u}}_h, \widehat{\boldsymbol{\sigma}}_h) \in [\mathcal{U}^h]^2 \times \mathcal{W}^h \times \mathcal{W}^h \times \mathcal{P}^h \times [\mathcal{M}_p^h]^2 \times [\mathcal{M}_u^h]^2$ such that

$$(S_h, \phi_h)_{0,\Omega} - B_h^*(\mathbf{u}_h, \phi_h) - D_h(\widehat{\mathbf{u}}_h, \phi_h) = 0, \tag{12a}$$

$$(S_h^\mu, \psi_h)_{0,\Omega} = (\mu(S_h)S_h, \psi_h)_{0,\Omega}, \tag{12b}$$

$$B_h(S_h^\mu, \mathbf{v}_h) - C_h(p_h, \mathbf{v}_h) - D_h^*(\widehat{\boldsymbol{\sigma}}_h, \mathbf{v}_h) = (\mathbf{f}, \mathbf{v}_h)_{0,\Omega}, \tag{12c}$$

$$C_h^*(\mathbf{u}_h, q_h) + D_h(\widehat{\mathbf{u}}_h, q_h \mathbf{I}_2) = 0, \tag{12d}$$

$$D_h^*(\widehat{\boldsymbol{\phi}}_h, \mathbf{u}_h) = 0, \tag{12e}$$

$$D_h(\widehat{\mathbf{v}}_h, S_h^\mu - p_h \mathbf{I}_2) = 0, \tag{12f}$$

for any test functions $(\phi_h, \psi_h, \mathbf{v}_h, q_h, \widehat{\boldsymbol{\phi}}_h, \widehat{\mathbf{v}}_h) \in \mathcal{W}^h \times \mathcal{W}^h \times [\mathcal{U}^h]^2 \times \mathcal{P}^h \times [\mathcal{M}_u^h]^2 \times [\mathcal{M}_p^h]^2$. The zero average condition for the approximate solution p_h , $\int_\Omega p_h \, dx = 0$ is also imposed to ensure the uniqueness of the solution. In the above formulation, the bilinear forms are defined as:

$$B_h(\phi_h, \mathbf{v}_h) = \int_\Omega \phi_h : \nabla_h \mathbf{v}_h \, dx - \sum_{e \in \mathcal{F}_p^N} \int_e [\phi_h \mathbf{n} \cdot \mathbf{v}_h] \, ds, \tag{13a}$$

$$B_h^*(\mathbf{v}_h, \phi_h) = - \int_\Omega \mathbf{v}_h \cdot \text{div}_h(\phi_h) \, dx + \sum_{e \in \mathcal{F}_u^D} \int_e [\phi_h \mathbf{n} \cdot \mathbf{v}_h] \, ds, \tag{13b}$$

$$C_h(q_h, \mathbf{v}_h) = \int_\Omega q_h \text{div}_h \mathbf{v}_h \, dx - \sum_{e \in \mathcal{F}_p^N} \int_e [q_h \mathbf{n} \cdot \mathbf{v}_h] \, ds, \tag{13c}$$

$$C_h^*(\mathbf{v}_h, q_h) = - \int_\Omega \mathbf{v}_h \cdot \nabla_h q_h \, dx + \sum_{e \in \mathcal{F}_u^D} \int_e [q_h \mathbf{n} \cdot \mathbf{v}_h] \, ds, \tag{13d}$$

$$D_h(\widehat{\mathbf{v}}_h, \phi_h) = \sum_{e \in \mathcal{F}_p^N} \int_e \widehat{\mathbf{v}}_h \cdot [\phi_h \mathbf{n}] \, ds, \tag{13e}$$

$$D_h^*(\widehat{\boldsymbol{\phi}}_h, \mathbf{v}_h) = \sum_{e \in \mathcal{F}_u^D} \int_e \widehat{\boldsymbol{\phi}}_h \cdot [\mathbf{v}_h] \, ds, \tag{13f}$$

where $[\phi \mathbf{n} \cdot \mathbf{v}]_e = (\phi^+ \mathbf{n}^+) \cdot \mathbf{v}^+ + (\phi^- \mathbf{n}^-) \cdot \mathbf{v}^-$, ∇_h and div_h are the elementwise gradient operator and elementwise divergence operator, respectively. Here, we remark that the bilinear form $C_h(q_h, \mathbf{v}_h)$ is closely related to $B_h(\phi_h, \mathbf{v}_h)$. It can be easily verified that

$$\begin{aligned} C_h(q_h, \mathbf{v}_h) &= \int_\Omega q_h \text{div}_h \mathbf{v}_h \, dx - \sum_{e \in \mathcal{F}_p^N} \int_e [q_h \mathbf{n} \cdot \mathbf{v}_h] \, ds \\ &= \int_\Omega q_h \mathbf{I}_2 : \nabla_h \mathbf{v}_h \, dx - \sum_{e \in \mathcal{F}_p^N} \int_e [(q_h \mathbf{I}_2) \mathbf{n} \cdot \mathbf{v}_h] \, ds = B_h(q_h \mathbf{I}_2, \mathbf{v}_h) \end{aligned}$$

$$\begin{aligned} \text{Similarly, } C_h^*(\mathbf{v}_h, q_h) &= - \int_\Omega \mathbf{v}_h \cdot \nabla_h q_h \, dx + \sum_{e \in \mathcal{F}_u^D} \int_e [q_h \mathbf{n} \cdot \mathbf{v}_h] \, ds \\ &= - \int_\Omega \mathbf{v}_h \cdot \text{div}_h(q_h \mathbf{I}_2) \, dx + \sum_{e \in \mathcal{F}_u^D} \int_e [(q_h \mathbf{I}_2) \mathbf{n} \cdot \mathbf{v}_h] \, ds = B_h^*(\mathbf{v}_h, q_h \mathbf{I}_2). \end{aligned}$$

Therefore, in some situations, we will use $B_h(q_h \mathbf{I}_2, \mathbf{v}_h)$ instead of $C_h(q_h, \mathbf{v}_h)$ without further explanation.

2.4 Solution Algorithm

After an introduction of some matrix representations of the bilinear forms, we can present the equations of (12) in a more compact way. We use the notation $m_{v_h}, m_{\phi_h}, m_{q_h}, m_{\widehat{v}_h}$ and $m_{\widehat{\phi}_h}$ to denote the dimensions of $[\mathcal{U}^h]^2, \mathcal{W}^h, \mathcal{P}^h, [\mathcal{M}_p^h]^2$ and $[\mathcal{M}_u^h]^2$, respectively.

Furthermore, we let the basis functions of the corresponding finite element spaces as $\{v_i\}_{i=1}^{m_{v_h}}, \{\phi_i\}_{i=1}^{m_{\phi_h}}, \{q_i\}_{i=1}^{m_{q_h}}, \{\widehat{v}_i\}_{i=1}^{m_{\widehat{v}_h}}$ and $\{\widehat{\phi}_i\}_{i=1}^{m_{\widehat{\phi}_h}}$, respectively. So we can write the approximate solutions as a linear combinations of the basis functions as below

$$\begin{aligned}
 \mathbf{u}_h &= \sum_{i=1}^{m_{v_h}} u_i v_i, & S_h &= \sum_{i=1}^{m_{\phi_h}} S_i \phi_i, & S_h^\mu &= \sum_{i=1}^{m_{\phi_h}} S_i^\mu \phi_i, \\
 p_h &= \sum_{i=1}^{m_{q_h}} p_i q_i, & \widehat{\mathbf{u}}_h &= \sum_{i=1}^{m_{\widehat{v}_h}} \widehat{u}_i \widehat{v}_i, & \widehat{\sigma}_h &= \sum_{i=1}^{m_{\widehat{\phi}_h}} \widehat{\sigma}_i \widehat{\phi}_i.
 \end{aligned}$$

Then, we define the matrix representations of the bilinear forms as follows:

$$\begin{aligned}
 (B)_{ij} &= B_h(\phi_j, v_i), & (B^*)_{ij} &= B_h^*(v_j, \phi_i), \\
 (C)_{ij} &= C_h(q_j, v_i), & (C^*)_{ij} &= C_h^*(v_j, q_i), \\
 (D)_{ij} &= D_h(\widehat{v}_j, \phi_i), & (D^*)_{ij} &= D_h^*(\widehat{\phi}_j, v_i), \\
 (E)_{ij} &= D_h(\widehat{v}_j, q_i \mathbf{I}_2), & (M)_{ij} &= (\phi_j, \phi_i)_{0,\Omega}.
 \end{aligned}$$

For the purpose of clarification, we will use the notation $\vec{\mathbf{u}}_h$ to represent the coefficient vector $(u_1, u_2, \dots, u_{m_{v_h}})^T$ of the finite element solution \mathbf{u}_h , and the notation is similar for the remaining approximate solutions. Note, using integration by parts, we can show that $B_h(\phi_j, v_i) = B_h^*(v_j, \phi_j)$, so these bilinear forms are adjoint to each other and we have $B^T = B^*$ and $C^T = C^*$. Then, the equations in (12) can be rewritten into the following algebraic system of equations:

$$\begin{aligned}
 M \vec{S}_h - B^T \vec{\mathbf{u}}_h - D \vec{\widehat{\mathbf{u}}}_h &= 0 \\
 M \vec{S}_h^\mu &= \mathbf{F}(\vec{S}_h) \\
 B \vec{S}_h^\mu - C \vec{p}_h - D^* \vec{\widehat{\sigma}}_h &= \mathbf{f}_h \\
 C^T \vec{\mathbf{u}}_h + E \vec{\widehat{\mathbf{u}}}_h &= 0 \\
 (D^*)^T \vec{\mathbf{u}}_h &= 0 \\
 D^T \vec{S}_h^\mu - E^T \vec{p}_h &= 0
 \end{aligned} \tag{14}$$

where $\mathbf{f}_h = \left((f, v_1)_{0,\Omega}, (f, v_2)_{0,\Omega}, \dots, (f, v_{m_{v_h}})_{0,\Omega} \right)^T$ and similar for $\mathbf{g}_{h,D}$ and $\mathbf{g}_{h,N}$.

Here, we emphasize that $\mathbf{F}(\vec{S}_h)$ is a vector-valued function depends on the approximate solution $S_h = \sum_{i=1}^{m_{\phi_h}} S_i \phi_i$ and is defined entrywise as

$$\mathbf{F}(\vec{S}_h)_j = (\mu(S_h) S_h, \phi_j)_{0,\Omega}.$$

Here, we eliminate the variable \vec{S}_h^μ by rewriting it as

$$\vec{S}_h^\mu = M^{-1} \mathbf{F}(\vec{S}_h).$$

Then, the matrix system becomes

$$\begin{pmatrix} M & -B^T & 0 & 0 & -D \\ BM^{-1}F & 0 & -C & -D^* & 0 \\ 0 & C^T & 0 & 0 & E \\ 0 & (D^*)^T & 0 & 0 & 0 \\ D^T M^{-1}F & 0 & -E^T & 0 & 0 \end{pmatrix} \begin{pmatrix} \vec{S}_h \\ \vec{u}_h \\ \vec{p}_h \\ \vec{\sigma}_h \\ \vec{u}_h \end{pmatrix} = \begin{pmatrix} 0 \\ f_h \\ 0 \\ 0 \\ 0 \end{pmatrix} \tag{15}$$

where F is a matrix function depends on \vec{S}_h .

It is clear that $F(\vec{S}_h)$ is a nonlinear function, so we choose to use the Newton’s method for solving the resulting system (15). Then, we introduce the notation of variables for the iterations of the Newton’s method as follows:

In the n -th iteration, let $y_h^n = \begin{pmatrix} \vec{S}_h^n \\ \vec{u}_h^n \\ \vec{p}_h^n \\ \vec{\sigma}_h^n \\ \vec{u}_h^n \end{pmatrix}$ be the solution vector and

$$H(y_h^n) = \begin{pmatrix} M\vec{S}_h^n - B^T\vec{u}_h^n - D\vec{u}_h^n \\ BM^{-1}F(\vec{S}_h^n) - C\vec{p}_h^n - D^*\vec{\sigma}_h^n - f_h \\ C^T\vec{u}_h^n + E\vec{u}_h^n \\ (D^*)^T\vec{u}_h^n \\ D^T M^{-1}F(\vec{S}_h^n) - E^T\vec{p}_h^n \end{pmatrix}$$

be the residual vector. The Jacobian matrix of $H(y_h^n)$ is

$$J(y_h^n) = \begin{pmatrix} M & -B^T & 0 & 0 & -D \\ BM^{-1}F'(\vec{S}_h^n) & 0 & -C & -D^* & 0 \\ 0 & C^T & 0 & 0 & E \\ 0 & (D^*)^T & 0 & 0 & 0 \\ D^T M^{-1}F'(\vec{S}_h^n) & 0 & -E^T & 0 & 0 \end{pmatrix}$$

where $F'(\vec{S}_h^n)$ is the derivative of $F(\vec{S}_h^n)$ with respect to \vec{S}_h^n , and $F'(\vec{S}_h^n)$ is defined element-wise as

$$F'(\vec{S}_h^n)_{ij} = (\mu(S_h^n)\phi_j, \phi_i)_{0,\Omega} + \left(\frac{\partial \mu(S_h^n)}{\partial S_j^n} S_h^n, \phi_i \right)_{0,\Omega}.$$

We remark that one can implement the inversion of the matrix $J(y_h^n)$ efficiently by hybridization.

Finally, our algorithm can be concluded as follows:

Step 1 Seek an initial guess y_h^0 for the Newton’s method by solving (15) with $\mu(S_h) = 1$, i.e., $BM^{-1}F$ and $DM^{-1}F$ are replaced by B and D , respectively, in the matrix system (15).

Step 2 Solve the nonlinear system (15) by the Newton’s method. In other words, we update the solution iteratively as

$$y_h^{n+1} = y_h^n - J(y_h^n)^{-1}H(y_h^n).$$

Step 3 The iterative process stops until the successive error between u_h^{n+1} and u_h^n is small enough.

2.5 Postprocessing

Due to the relationship between the SDG method and the HDG method (see [6] for details), the SDG method enjoys a superconvergence error estimates of the velocity variable after postprocessing of the approximate solution \mathbf{u}_h . As we have mentioned that all the variables in our method converges optimally with respect to the L^2 -norm, so now the postprocessing results can further improve the velocity solution and the postprocessed solution converges with order $k + 2$ by using polynomials of degree $k \geq 1$ for approximation.

The postprocessing procedure is performed locally, so the computation is in an efficient element-by-element fashion. Hence, the computational cost is smaller than solving the original solution. Here, we remark that the postprocessed velocity \mathbf{u}_h^* is divergence-free and is $H(\text{div})$ -conforming, this nice property is suitable for linearizing the Navier–Stokes equations and deriving a consistent and stable numerical scheme for solving the equations (see [5]).

In our method, the local postprocessing is performed on each $S(v)$ such that for any edge $e \in \partial S(v)$, the postprocessed velocity $\mathbf{u}_h^* \in [P^{k+1}(S(v))]^2$ satisfies

$$\int_e (\mathbf{u}_h^* - \mathbf{u}_h) \cdot \mathbf{n} \widehat{\boldsymbol{\phi}}_h \, ds = 0 \quad \forall \widehat{\boldsymbol{\phi}}_h \in P^k(e),$$

and

$$\int_e \left((\mathbf{n} \times \nabla)(\mathbf{u}_h^*) - \mathbf{n} \times (\{L_h^T\} \mathbf{n}) \right) (\mathbf{n} \times \nabla) \widehat{\boldsymbol{\phi}}_h \, ds = 0 \quad \forall \widehat{\boldsymbol{\phi}}_h \in P^k(e).$$

Here, $\mathbf{n} \times \nabla = n_2 \partial_1 - n_1 \partial_2$, L_h is the numerical solution of velocity gradient L and $\{L_h^T\}$ is the average of the transpose of L_h on the edge e , i.e., $\{L_h^T\} = \frac{(L_h^T)^+ + (L_h^T)^-}{2}$. Moreover, \mathbf{u}_h^* also satisfies

$$\int_{S(v)} (\mathbf{u}_h^* - \mathbf{u}_h) \cdot \nabla v_h \, dx = 0 \quad \forall v_h \in P^k(S(v)),$$

and

$$\int_{S(v)} (\nabla \times \mathbf{u}_h^* - \mathcal{L}_h) v_h \mathcal{B} \, dx = 0 \quad \forall v_h \in P^{k-1}(S(v)),$$

where $\mathcal{L}_h = (L_h)_{21} - (L_h)_{12}$ and \mathcal{B} is the bubble function defined by the product of the barycentric coordinates of vertices of $S(v)$.

We remark that as L_h is not a fundamental variable in (12), so it cannot be obtained directly from our proposed scheme and a posteriori differentiation on \mathbf{u}_h is performed to acquire the numerical gradient.

2.6 On the Slip Boundary Condition

In this section, we present a modification of our numerical scheme when the slip boundary condition is imposed in the system (1). In particular, we consider the system

$$\begin{aligned} -\operatorname{div}(\mu \boldsymbol{\varepsilon}(\mathbf{u}) - p \mathbf{I}_2) &= \mathbf{f} && \text{in } \Omega, \\ \operatorname{div} \mathbf{u} &= 0 && \text{in } \Omega, \\ \mathbf{u} \cdot \mathbf{n} &= 0 && \text{on } \partial \Omega, \\ (\mu \boldsymbol{\varepsilon}(\mathbf{u}) \mathbf{n}) \cdot \mathbf{t} &= \alpha \mathbf{u} \cdot \mathbf{t} && \text{on } \partial \Omega, \end{aligned} \tag{16}$$

where \mathbf{t} is the unit tangential vector defined on $\partial\Omega$ and α is a constant. The corresponding first order form is written as

$$S = \varepsilon(\mathbf{u}) \quad \text{in } \Omega, \tag{17a}$$

$$S^\mu = \mu(S)S \quad \text{in } \Omega, \tag{17b}$$

$$-\operatorname{div} S^\mu + \nabla p = \mathbf{f} \quad \text{in } \Omega, \tag{17c}$$

$$\operatorname{div} \mathbf{u} = 0 \quad \text{in } \Omega, \tag{17d}$$

$$\mathbf{u} \cdot \mathbf{n} = 0 \quad \text{on } \partial\Omega, \tag{17e}$$

$$(\mu \varepsilon(\mathbf{u})\mathbf{n}) \cdot \mathbf{t} = \alpha \mathbf{u} \cdot \mathbf{t} \quad \text{on } \partial\Omega. \tag{17f}$$

There are multiple ways to impose the boundary conditions (17e) and (17f), and we will consider a standard approach. In particular, we will impose the condition (17e) in the approximation space for \mathbf{u} and the condition (17f) by the variational formulation. To impose the condition (17f), we multiply the equation (17c) by a test function \mathbf{v}_h and integrate the resulting equation on a triangle τ to get

$$\int_\tau S^\mu : \nabla \mathbf{v}_h \, dx - \int_{\partial\tau} (S^\mu \mathbf{n}) \cdot \mathbf{v}_h \, ds - \int_\tau p \operatorname{div}(\mathbf{v}_h) \, dx + \int_{\partial\tau} (\mathbf{p}\mathbf{n}) \cdot \mathbf{v}_h \, ds = \int_\tau \mathbf{f} \cdot \mathbf{v}_h \, dx.$$

where we assume one of the edges of τ lies on the domain boundary $\partial\Omega$. We further write the above equation as

$$\begin{aligned} &\int_\tau S^\mu : \nabla \mathbf{v}_h \, dx - \int_{\partial\tau \setminus \partial\Omega} (S^\mu \mathbf{n}) \cdot \mathbf{v}_h \, ds - \int_\tau p \operatorname{div}(\mathbf{v}_h) \, dx + \int_{\partial\tau \setminus \partial\Omega} (\mathbf{p}\mathbf{n}) \cdot \mathbf{v}_h \, ds \\ &- \int_{\partial\tau \cap \partial\Omega} (S^\mu \mathbf{n}) \cdot \mathbf{v}_h \, ds + \int_{\partial\tau \cap \partial\Omega} (\mathbf{p}\mathbf{n}) \cdot \mathbf{v}_h \, ds = \int_\tau \mathbf{f} \cdot \mathbf{v}_h \, dx. \end{aligned} \tag{18}$$

Since the test function \mathbf{v}_h satisfies $\mathbf{v}_h \cdot \mathbf{n} = 0$ on $\partial\Omega$, we have

$$\int_{\partial\tau \cap \partial\Omega} (\mathbf{p}\mathbf{n}) \cdot \mathbf{v}_h \, ds = \int_{\partial\tau \cap \partial\Omega} (\mathbf{p}\mathbf{n}) \cdot (\mathbf{v}_h \cdot \mathbf{n})\mathbf{n} \, ds + \int_{\partial\tau \cap \partial\Omega} (\mathbf{p}\mathbf{n}) \cdot (\mathbf{v}_h \cdot \mathbf{t})\mathbf{t} \, ds = 0,$$

and

$$\begin{aligned} \int_{\partial\tau \cap \partial\Omega} (S^\mu \mathbf{n}) \cdot \mathbf{v}_h \, ds &= \int_{\partial\tau \cap \partial\Omega} (S^\mu \mathbf{n}) \cdot (\mathbf{v}_h \cdot \mathbf{n})\mathbf{n} \, ds + \int_{\partial\tau \cap \partial\Omega} (S^\mu \mathbf{n}) \cdot (\mathbf{v}_h \cdot \mathbf{t})\mathbf{t} \, ds \\ &= \int_{\partial\tau \cap \partial\Omega} (S^\mu \mathbf{n}) \cdot (\mathbf{v}_h \cdot \mathbf{t})\mathbf{t} \, ds. \end{aligned}$$

So, we can write (18) as

$$\begin{aligned} &\int_\tau S^\mu : \nabla \mathbf{v}_h \, dx - \int_{\partial\tau \setminus \partial\Omega} (S^\mu \mathbf{n}) \cdot \mathbf{v}_h \, ds - \int_\tau p \operatorname{div}(\mathbf{v}_h) \, dx + \int_{\partial\tau \setminus \partial\Omega} (\mathbf{p}\mathbf{n}) \cdot \mathbf{v}_h \, ds \\ &- \int_{\partial\tau \cap \partial\Omega} (S^\mu \mathbf{n}) \cdot (\mathbf{v}_h \cdot \mathbf{t})\mathbf{t} \, ds = \int_\tau \mathbf{f} \cdot \mathbf{v}_h \, dx. \end{aligned} \tag{19}$$

Hence, we can impose the boundary condition (17f) in the following way

$$\begin{aligned} &\int_\tau S^\mu : \nabla \mathbf{v}_h \, dx - \int_{\partial\tau \setminus \partial\Omega} (S^\mu \mathbf{n}) \cdot \mathbf{v}_h \, ds - \int_\tau p \operatorname{div}(\mathbf{v}_h) \, dx + \int_{\partial\tau \setminus \partial\Omega} (\mathbf{p}\mathbf{n}) \cdot \mathbf{v}_h \, ds \\ &- \int_{\partial\tau \cap \partial\Omega} \alpha(\mathbf{u} \cdot \mathbf{t})(\mathbf{v}_h \cdot \mathbf{t}) \, ds = \int_\tau \mathbf{f} \cdot \mathbf{v}_h \, dx. \end{aligned} \tag{20}$$

3 Analysis for the Discrete Problem

Before we start the proof of the stability and the optimal convergence of the proposed numerical scheme, due to the staggered continuity conditions inherited from the SDG method, many nice properties are retained and we will introduce them in this section.

3.1 SDG Results

For simplicity, we assume $\partial\Omega_D = \partial\Omega$ and $\mathbf{g}_D = \mathbf{0}$ in our proof. Nevertheless, we remark here that our method can be extended to mixed boundary cases. In the SDG method, the finite element spaces with staggered continuities are defined as

$$\begin{aligned} \mathcal{U}_c^h &= \left\{ v : v|_\tau \in P^k(\tau), \forall \tau \in \mathcal{T}, v \text{ is continuous across } e \in \mathcal{F}_u^0, v|_{\partial\Omega} = 0 \right\}, \\ \mathcal{W}_c^h &= \left\{ \phi : \phi|_\tau \in [P^k(\tau)]^2, \forall \tau \in \mathcal{T}, \phi \cdot \mathbf{n}_e \text{ is continuous across } e \in \mathcal{F}_p \right\}, \\ \mathcal{P}_c^h &= \left\{ q : q|_\tau \in P^k(\tau), \forall \tau \in \mathcal{T}, q \text{ is continuous across } e \in \mathcal{F}_p \right\}, \end{aligned}$$

for the numerical solution of velocity, gradient and pressure, respectively.

We can observe that after imposing the staggered continuity conditions (5) and (6), the approximate velocity \mathbf{u}_h and stress tensor $\sigma_h = S_h^{\mu} - p_h \mathbf{I}_2$ in our numerical scheme (12) have the property that $\mathbf{u}_h \in [\mathcal{U}_c^h]^2$ and $\sigma_h \in [\mathcal{W}_c^h]^2$. Therefore, we can make use of the SDG related theorems in our analysis.

We first define some norms in the finite element spaces mentioned above. In the space \mathcal{U}_c^h , we define the discrete L^2 -norm $\|\cdot\|_X$ and the discrete H^1 -norm $\|\cdot\|_Z$ as the following:

$$\begin{aligned} \|v_h\|_X^2 &= \int_{\Omega} v_h^2 \, dx + \sum_{e \in \mathcal{F}_u^0} h_e \int_e v_h^2 \, ds \\ \|v_h\|_Z^2 &= \int_{\Omega} |\nabla_h v_h|^2 \, dx + \sum_{e \in \mathcal{F}_p} h_e^{-1} \int_e [v_h]^2 \, ds. \end{aligned}$$

Here, the jump $[v_h]|_e$ for a scalar-valued function $v_h \in \mathcal{U}_c^h$ across an edge e is defined as

$$[v_h]|_e = (\mathbf{n}^+ \cdot \mathbf{n}_e) v_h^+ + (\mathbf{n}^- \cdot \mathbf{n}_e) v_h^-.$$

Similarly, the notation $\|\cdot\|_{X'}$ and $\|\cdot\|_{Z'}$ denotes the discrete L^2 -norm and H^1 -norm respectively in the space \mathcal{W}_c^h . The definition is

$$\begin{aligned} \|\phi_h\|_{X'}^2 &= \int_{\Omega} |\phi_h|^2 \, dx + \sum_{e \in \mathcal{F}_p} h_e \int_e (\phi_h \cdot \mathbf{n})^2 \, ds, \\ \|\phi_h\|_{Z'}^2 &= \int_{\Omega} (\nabla_h \cdot \phi_h)^2 \, dx + \sum_{e \in \mathcal{F}_u^0} h_e^{-1} \int_e [\phi_h \cdot \mathbf{n}]^2 \, ds, \end{aligned}$$

where the jump $[\phi_h \cdot \mathbf{n}]$ for a vector-valued function $\phi_h \in \mathcal{W}_c^h$ across an edge e is defined as

$$[\phi_h \cdot \mathbf{n}]|_e = \phi_h^+ \cdot \mathbf{n}^+ + \phi_h^- \cdot \mathbf{n}^-.$$

Note, the discrete L^2 -norm $\|\cdot\|_{X'}$ in \mathcal{W}_c^h is equivalent to the standard L^2 -norm $\|\cdot\|_{0,\Omega}$ (see [8] for details), i.e., for any $\phi_h \in \mathcal{W}_c^h$, there exists a positive constant k_W , independent of

the mesh size h , such that

$$k_W \|\boldsymbol{\phi}_h\|_{X'} \leq \|\boldsymbol{\phi}_h\|_{0,\Omega} \leq \|\boldsymbol{\phi}_h\|_{X'}. \tag{21}$$

Last, we define the norm $\|\cdot\|_P$ in \mathcal{P}_c^h as

$$\|q_h\|_P = \int_{\Omega} q_h^2 dx + \sum_{e \in \mathcal{F}_p} h_e \int_e q_h^2 ds.$$

Similarly, the discrete L^2 -norm $\|\cdot\|_P$ in \mathcal{P}_c^h is equivalent to the standard L^2 -norm $\|\cdot\|_{0,\Omega}$, i.e., for any $q_h \in \mathcal{P}_c^h$, there exists a positive constant k_P , independent of the mesh size h , such that

$$k_P \|q_h\|_P \leq \|q_h\|_{0,\Omega} \leq \|q_h\|_P. \tag{22}$$

Here we remark that the approximate solution $\mathbf{u}_h = (u_{h,1}, u_{h,2})^T$ in our numerical scheme lies in the product space $[\mathcal{U}_c^h]^2$, but we still use the notation $\|\cdot\|_X$ to denote the discrete L^2 -norm in $[\mathcal{U}_c^h]^2$ to avoid redundant notation. And the definition is

$$\|\mathbf{u}_h\|_X^2 = \|u_{h,1}\|_X^2 + \|u_{h,2}\|_X^2,$$

for which norm is used will be stated clearly in the context. Similarly, for the other discrete norms in different spaces, we use the same way to define the corresponding discrete norms in product spaces.

We are now ready to state the important theorems related to the SDG method, and the details of proof can be found in [9].

First, for any $v_h \in \mathcal{U}_c^h$ and $\boldsymbol{\phi}_h \in \mathcal{W}_c^h$, we can define two bilinear forms as

$$b_h(\boldsymbol{\phi}_h, v_h) = \int_{\Omega} \boldsymbol{\phi}_h \cdot \nabla_h v_h dx - \sum_{e \in \mathcal{F}_p} \int_e \boldsymbol{\phi}_h \cdot \mathbf{n} [v_h] ds,$$

$$b_h^*(v_h, \boldsymbol{\phi}_h) = - \int_{\Omega} v_h \cdot \operatorname{div}_h(\boldsymbol{\phi}_h) dx + \sum_{e \in \mathcal{F}_u^0} \int_e v_h [\boldsymbol{\phi}_h \cdot \mathbf{n}] ds,$$

then we can observe that for any $\mathbf{v}_h = (v_{h,1}, v_{h,2})^T \in [\mathcal{U}_c^h]^2$ and $\boldsymbol{\phi}_h = (\boldsymbol{\phi}_{h,1}, \boldsymbol{\phi}_{h,2})^T \in [\mathcal{W}_c^h]^2$, the bilinear form $B_h(\boldsymbol{\phi}_h, \mathbf{v}_h)$ coincides with $b_h(\boldsymbol{\phi}_{h,i}, v_{h,i})$ and $B_h^*(\mathbf{v}_h, \boldsymbol{\phi}_h)$ coincides with $b_h^*(v_{h,i}, \boldsymbol{\phi}_{h,i})$ in a way that

$$B_h(\boldsymbol{\phi}_h, \mathbf{v}_h) = \sum_{i=1}^2 b_h(\boldsymbol{\phi}_{h,i}, v_{h,i}),$$

$$B_h^*(\mathbf{v}_h, \boldsymbol{\phi}_h) = \sum_{i=1}^2 b_h^*(v_{h,i}, \boldsymbol{\phi}_{h,i}).$$

Therefore, the nice properties of $b_h(\boldsymbol{\phi}_{h,i}, v_{h,i})$ and $b_h^*(v_{h,i}, \boldsymbol{\phi}_{h,i})$ can be extended to the bilinear forms $B_h(\boldsymbol{\phi}_h, \mathbf{v}_h)$ and $B_h^*(\mathbf{v}_h, \boldsymbol{\phi}_h)$. For any $\mathbf{v}_h \in [\mathcal{U}_c^h]^2$ and $\boldsymbol{\phi}_h \in [\mathcal{W}_c^h]^2$, these properties can be summarized as

1. (Discrete adjoint condition)

$$B_h(\boldsymbol{\phi}_h, \mathbf{v}_h) = B_h^*(\mathbf{v}_h, \boldsymbol{\phi}_h). \tag{23}$$

2. (Continuity conditions)

$$|B_h(\phi_h, \mathbf{v}_h)| \leq \|\phi_h\|_{X'} \|\mathbf{v}_h\|_Z, \tag{24a}$$

$$|B_h^*(\mathbf{v}_h, \phi_h)| \leq \|\mathbf{v}_h\|_X \|\phi_h\|_{Z'}. \tag{24b}$$

3. (Inf-sup conditions) There exists two positive constants β_1 and β_2 , both are independent of h , such that

$$\inf_{\mathbf{v}_h \in [\mathcal{W}_c^h]^2 \setminus \{0\}} \sup_{\phi_h \in [\mathcal{W}_c^h]^2 \setminus \{0\}} \frac{B_h(\phi_h, \mathbf{v}_h)}{\|\phi_h\|_{X'} \|\mathbf{v}_h\|_Z} \geq \beta_1, \tag{25a}$$

$$\inf_{\phi_h \in [\mathcal{W}_c^h]^2 \setminus \{0\}} \sup_{\mathbf{v}_h \in [\mathcal{U}_c^h]^2 \setminus \{0\}} \frac{B_h^*(\mathbf{v}_h, \phi_h)}{\|\mathbf{v}_h\|_X \|\phi_h\|_{Z'}} \geq \beta_2. \tag{25b}$$

Similarly, the bilinear form (13c) also has these good properties as (13a) and (13b).

Lemma 1 For any $\mathbf{v}_h \in [\mathcal{U}_c^h]^2$ and $q_h \in \mathcal{P}_c^h$, we have

1. (Discrete adjoint condition)

$$C_h(q_h, \mathbf{v}_h) = C_h^*(\mathbf{v}_h, q_h). \tag{26}$$

2. (Continuity condition)

$$|C_h(q_h, \mathbf{v}_h)| \leq \|q_h\|_P \|\mathbf{v}_h\|_Z. \tag{27}$$

3. (Inf-sup condition) There exist a positive constant γ , independent of the mesh size h , such that

$$\inf_{\mathbf{v}_h \in [\mathcal{U}_c^h]^2 \setminus \{0\}} \sup_{q_h \in \mathcal{P}_c^h \setminus \{0\}} \frac{C_h(q_h, \mathbf{v}_h)}{\|q_h\|_P \|\mathbf{v}_h\|_Z} \geq \gamma. \tag{28}$$

The discrete adjoint condition (26) and the continuity condition (27) follow from (23) and the Cauchy–Schwarz inequality, respectively. And using the fact that $C_h(q_h, \mathbf{v}_h) = B_h(q_h \mathbf{I}_2, \mathbf{v}_h)$, the proof of the inf-sup condition (28) is just the generalization of the proof of (25a) in [9].

3.2 Interpolation Operators

From the inf-sup conditions, we can define some interpolation operators, which are vital for the analysis of the convergence estimates of our numerical scheme (see [12] for more general theory).

First, the inf-sup condition (25b) implies that there exists an operator $\mathcal{I} : [H^1(\Omega)]^2 \rightarrow [\mathcal{U}_c^h]^2$ such that for any $\mathbf{u} \in [H^1(\Omega)]^2$

$$B_h^*(\mathcal{I}\mathbf{u} - \mathbf{u}, \psi_h) = 0 \quad \forall \psi_h \in [\mathcal{W}_c^h]^2. \tag{29}$$

Furthermore, if $\mathbf{u} \in [H^{k+1}(\Omega)]^2$, we have the following interpolation error estimate for the operators \mathcal{I} : there exists a positive constant C_I , independent of the mesh size h , such that

$$\|\mathbf{u} - \mathcal{I}\mathbf{u}\|_{0,\Omega} \leq C_I h^{k+1} |\mathbf{u}|_{[H^{k+1}(\Omega)]^2}. \tag{30}$$

Besides this interpolation operator \mathcal{I} , we will then construct another operator $\mathcal{J} : [H(\mathbf{div}; \Omega)]^2 \rightarrow [\mathcal{W}_c^h]^2$ with a property that \mathcal{J} is symmetry preserving. We first define an approximation space for skew-symmetric matrix as follows:

$$\mathcal{K}^h = \{\eta : \eta|_\tau \in [P^k(\tau)]^{2 \times 2}, \forall \tau \in \mathcal{T}, \eta = -\eta^T\}.$$

And for any $(\phi_h, \mathbf{v}_h, \eta_h) \in [\mathcal{W}_c^h]^2 \times [\mathcal{U}_c^h]^2 \times \mathcal{K}^h$, we define

$$\tilde{B}_h(\phi_h; \mathbf{v}_h, \eta_h) = B_h(\phi_h, \mathbf{v}_h) - \int_{\Omega} \phi_h : \eta_h \, dx$$

and

$$\|(\mathbf{v}_h, \eta_h)\|_{\tilde{Z}}^2 = \int_{\Omega} |\eta_h - \nabla_h \mathbf{v}_h|^2 \, dx + \sum_{e \in \mathcal{F}_p} h_e^{-1} \int_e |[\mathbf{v}_h]|^2 \, ds.$$

Then, from the results in [22], we can state an inf-sup condition regarding the bilinear form $\tilde{B}_h(\phi_h; \mathbf{v}_h, \eta_h)$ as below: there exists a positive constant β_3 , independent of the mesh size h , such that

$$\inf_{(\mathbf{v}_h, \eta_h) \in [\mathcal{U}_c^h]^2 \times \mathcal{K}^h \setminus \{(\mathbf{0}, 0)\}} \sup_{\phi_h \in [\mathcal{W}_c^h]^2 \setminus \{0\}} \frac{\tilde{B}_h(\phi_h; \mathbf{v}_h, \eta_h)}{\|\phi_h\|_{X'} \|(\mathbf{v}_h, \eta_h)\|_{\tilde{Z}}} \geq \beta_3.$$

This inf-sup condition implies that given $\phi \in [H(\mathbf{div}; \Omega)]^2$, there exists a unique solution $(\tilde{\phi}_h, \tilde{\mathbf{v}}_h, \tilde{\eta}_h) \in [\mathcal{W}_c^h]^2 \times [\mathcal{U}_c^h]^2 \times \mathcal{K}^h$ such that for any $(\phi_h, \mathbf{v}_h, \eta_h) \in [\mathcal{W}_c^h]^2 \times [\mathcal{U}_c^h]^2 \times \mathcal{K}^h$

$$\begin{aligned} \int_{\Omega} \tilde{\phi}_h : \phi_h \, dx + \tilde{B}_h(\phi_h; \tilde{\mathbf{v}}_h, \tilde{\eta}_h) &= \int_{\Omega} \phi : \phi_h \, dx, \\ \tilde{B}_h(\tilde{\phi}_h; \mathbf{v}_h, \eta_h) &= \tilde{B}_h(\phi; \mathbf{v}_h, \eta_h). \end{aligned} \tag{31}$$

Therefore, the operator $\mathcal{J} : [H(\mathbf{div}; \Omega)]^2 \rightarrow [\mathcal{W}_c^h]^2$ is defined as $\mathcal{J}\phi = \tilde{\phi}_h \in [\mathcal{W}_c^h]^2$ for any $\phi \in [H(\mathbf{div}; \Omega)]^2$. Here, $\tilde{\phi}_h$ is the solution of the system (31) and from the definition of \mathcal{J} , we have

$$\tilde{B}_h(\mathcal{J}\phi - \phi; \mathbf{v}_h, \eta_h) = 0 \quad \forall (\mathbf{v}_h, \eta_h) \in [\mathcal{U}_c^h]^2 \times \mathcal{K}^h. \tag{32}$$

Finally, we present two lemmas to show the interpolation error and symmetry preserving property of \mathcal{J} .

Lemma 2 (Stability and interpolation error for \mathcal{J}) *For any $\phi \in [H(\mathbf{div}; \Omega)]^2$, we have*

$$\|\mathcal{J}\phi\|_{X'} \leq C \|\phi\|_{[H(\mathbf{div}; \Omega)]^2}. \tag{33}$$

And if $\phi \in [H^{k+1}(\Omega)]^{2 \times 2}$, we have

$$\|\phi - \mathcal{J}\phi\|_{0, \Omega} \leq C_J h^{k+1} |\phi|_{[H^{k+1}(\Omega)]^{2 \times 2}}. \tag{34}$$

Here, C and C_J are some positive constants independent of the mesh size h .

Proof First, the inf-sup condition (25a) is equivalent to the following (see [28] for details): there exists a positive constant β'_1 , independent of the mesh size h , such that

$$\inf_{\phi_h \in [\mathcal{W}_c^h]^2 \setminus \{0\}} \sup_{\mathbf{v}_h \in [\mathcal{U}_c^h]^2 \setminus \{0\}} \frac{B_h(\phi_h, \mathbf{v}_h)}{\|\phi_h\|_{X'} \|\mathbf{v}_h\|_Z} \geq \beta'_1. \tag{35}$$

Since $\mathcal{J}\phi \in [\mathcal{W}_c^h]^2$, so the above inf-sup condition (35) implies

$$\begin{aligned} \|\mathcal{J}\phi\|_{X'} &\leq \frac{1}{\beta'_1} \sup_{\mathbf{v}_h \in [\mathcal{U}_c^h]^2 \setminus \{0\}} \frac{B_h(\mathcal{J}\phi, \mathbf{v}_h)}{\|\mathbf{v}_h\|_Z} \\ &= \frac{1}{\beta'_1} \sup_{\mathbf{v}_h \in [\mathcal{U}_c^h]^2 \setminus \{0\}} \frac{\tilde{B}_h(\mathcal{J}\phi; \mathbf{v}_h, 0)}{\|\mathbf{v}_h\|_Z} \end{aligned}$$

$$\begin{aligned} &= \frac{1}{\beta_1'} \sup_{\mathbf{v}_h \in [\mathcal{U}_c^h]^2 \setminus \{\mathbf{0}\}} \frac{\tilde{B}_h(\phi; \mathbf{v}_h, 0)}{\|\mathbf{v}_h\|_Z} \\ &= \frac{1}{\beta_1'} \sup_{\mathbf{v}_h \in [\mathcal{U}_c^h]^2 \setminus \{\mathbf{0}\}} \frac{B_h(\phi, \mathbf{v}_h)}{\|\mathbf{v}_h\|_Z} \\ &\leq \frac{\|\phi\|_{X'}}{\beta_1'} \leq C \|\phi\|_{[H(\mathbf{div}; \Omega)]^2}, \end{aligned}$$

where we have used the Eq. (32) and the continuity condition (24a) of the bilinear form $B_h(\phi_h, \mathbf{v}_h)$.

To show the interpolation error estimate, we consider the system (31) again and notice that for any $\psi_h \in [\mathcal{W}_c^h]^2$ and $(\phi_h, \mathbf{v}_h, \eta_h) \in [\mathcal{W}_c^h]^2 \times [\mathcal{U}_c^h]^2 \times \mathcal{K}^h$, we have

$$\begin{aligned} \int_{\Omega} (\mathcal{J}\phi - \psi_h) : \phi_h \, dx + \tilde{B}_h(\phi_h; \tilde{\mathbf{v}}_h, \tilde{\eta}_h) &= \int_{\Omega} (\phi - \psi_h) : \phi_h \, dx, \\ \tilde{B}_h(\mathcal{J}\phi - \psi_h; \mathbf{v}_h, \eta_h) &= \tilde{B}_h(\phi - \psi_h; \mathbf{v}_h, \eta_h). \end{aligned}$$

However, due to the uniqueness of the solution of the above system, we can conclude that

$$\|\mathcal{J}\phi - \psi_h\|_{X'} = \|\mathcal{J}(\phi - \psi_h)\|_{X'} \leq \frac{1}{\beta_1'} \|\phi - \psi_h\|_{X'}.$$

Therefore, the desired interpolation error follows by taking ψ_h as the standard conforming interpolant of ϕ for the triangulation \mathcal{T} and using the norm equivalence relation (21) in the following estimate:

$$\|\phi - \mathcal{J}\phi\|_{X'} \leq \|\phi - \psi_h\|_{X'} + \|\psi_h - \mathcal{J}\phi\|_{X'} \leq \left(\frac{1}{\beta_1'} + 1\right) \|\phi - \psi_h\|_{X'}.$$

□

From the definition of the interpolation operator \mathcal{J} and bilinear form $\tilde{B}_h(\phi_h; \mathbf{v}_h, \eta_h)$, we can rewrite the definition of \mathcal{J} through the bilinear form $B_h(\phi_h, \mathbf{v}_h)$ instead, and the symmetry preserving property can be then shown.

Lemma 3 For any $\phi \in [H(\mathbf{div}; \Omega)]^2$, we have

$$B_h(\mathcal{J}\phi - \phi, \mathbf{v}_h) = 0 \quad \forall \mathbf{v}_h \in [\mathcal{U}_c^h]^2. \tag{36}$$

Furthermore, if $\phi = \phi^T$, then $\mathcal{J}\phi = (\mathcal{J}\phi)^T$.

Proof Considering $\eta_h = 0$ in the Eq. (32), we immediately see (36) by the definition of $\tilde{B}_h(\phi_h; \mathbf{v}_h, \eta_h)$ as below

$$B_h(\mathcal{J}\phi - \phi, \mathbf{v}_h) = \tilde{B}_h(\mathcal{J}\phi - \phi; \mathbf{v}_h, 0) = 0 \quad \forall \mathbf{v}_h \in [\mathcal{U}_c^h]^2.$$

To show the symmetry preserving property, we take $\mathbf{v}_h = \mathbf{0}$ in the Eq. (32)

$$-\int_{\Omega} (\mathcal{J}\phi - \phi) : \eta_h \, dx = \tilde{B}_h(\mathcal{J}\phi - \phi; \mathbf{0}, \eta_h) = 0 \quad \forall \eta_h \in \mathcal{K}^h.$$

Since ϕ is assumed to be symmetric and η_h is skew-symmetric, so

$$\int_{\Omega} \mathcal{J}\phi : \eta_h \, dx = \int_{\Omega} \phi : \eta_h \, dx = 0 \quad \forall \eta_h \in \mathcal{K}^h$$

implies $\mathcal{J}\phi$ is also symmetric. □

4 Stability and Optimal Convergence Analysis

We will prove the stability and the optimal convergence of the proposed numerical scheme.

Theorem 1 *Let $(\mathbf{u}_h, S_h, S_h^\mu, p_h) \in [\mathcal{U}^h]^2 \times \mathcal{W}^h \times \mathcal{W}^h \times \mathcal{P}^h$ be the solutions of the numerical scheme (12), then the following stability estimates hold:*

$$\|\mathbf{u}_h\|_{0,\Omega} \leq \frac{C_P^2}{C_M \beta_1^2} \|\mathbf{f}\|_{0,\Omega}, \tag{37}$$

$$\|S_h\|_{0,\Omega} \leq \frac{C_P}{C_M \beta_1} \|\mathbf{f}\|_{0,\Omega}, \tag{38}$$

$$\|S_h^\mu\|_{0,\Omega} \leq \frac{C_P C_L}{C_M \beta_1} \|\mathbf{f}\|_{0,\Omega}, \tag{39}$$

$$\|p_h\|_{0,\Omega} \leq \frac{C_P}{\sqrt{2}} \left(\frac{1}{\beta_1'} + \frac{C_L}{C_M \beta_1} \right) \|\mathbf{f}\|_{0,\Omega}, \tag{40}$$

where β_1 and β_1' are the constants in (25a) and (35). And C_M, C_L and C_P are the constants that taken form the strongly monotone condition (3), the Lipschitz continuity condition (4), and the discrete Poincaré–Friedrichs inequality for piecewise H^1 functions, respectively. All these constants are independent of the mesh size h .

Proof Due to the staggered continuity conditions (5) and (6), we have the result that $\mathbf{u}_h \in [\mathcal{U}_c^h]^2, S_h^\mu - p_h \mathbf{I}_2 \in \mathcal{W}^h \cap [\mathcal{W}_c^h]^2$. Moreover, for any $\mathbf{v}_h \in [\mathcal{U}_c^h]^2, \phi_h \in [\mathcal{W}_c^h]^2, \widehat{\mathbf{v}}_h \in [\mathcal{M}_p^h]^2$ and $\widehat{\phi}_h \in [\mathcal{M}_u^h]^2$, we have

$$D_h^*(\widehat{\phi}_h, \mathbf{v}_h) = 0, \tag{41}$$

$$D_h(\widehat{\mathbf{v}}_h, \phi_h) = 0. \tag{42}$$

Therefore, if we take the test functions in (12) as the following:

$$\mathbf{v}_h = \mathbf{u}_h, \quad \phi_h = S_h^\mu, \quad \psi_h = -S_h, \quad q_h = p_h,$$

the system (12) reduces to

$$\begin{aligned} (S_h, S_h^\mu)_{0,\Omega} - B_h^*(\mathbf{u}_h, S_h^\mu) - D_h(\widehat{\mathbf{u}}_h, S_h^\mu) &= 0, \\ -(S_h^\mu, S_h)_{0,\Omega} &= -(\mu(S_h)S_h, S_h)_{0,\Omega}, \\ B_h(S_h^\mu, \mathbf{u}_h) - C_h(p_h, \mathbf{u}_h) - D_h^*(\widehat{\sigma}_h, \mathbf{u}_h) &= (\mathbf{f}, \mathbf{u}_h)_{0,\Omega}, \\ C_h^*(\mathbf{u}_h, p_h) + D_h(\widehat{\mathbf{u}}_h, p_h \mathbf{I}_2) &= 0. \end{aligned}$$

After summing up the above four equations and applying the discrete adjoint properties (23) and (26), we have

$$(\mu(S_h)S_h, S_h) = (\mathbf{f}, \mathbf{u}_h), \tag{43}$$

where we have used of the fact that $\mathbf{u}_h \in [\mathcal{U}_c^h]^2$ and $S_h^\mu - p_h \mathbf{I}_2 \in \mathcal{W}^h \cap [\mathcal{W}_c^h]^2$.

From the strongly monotone condition (3), and by the Cauchy–Schwarz inequality,

$$\|S_h\|_{0,\Omega}^2 \leq C_M^{-1} \|\mathbf{f}\|_{0,\Omega} \|\mathbf{u}_h\|_{0,\Omega}. \tag{44}$$

Now, the discrete Poincaré–Friedrichs inequality for piecewise H^1 functions (see [3]) implies that for any $\mathbf{v}_h \in \mathcal{U}^h$, there exists a positive constant C_P , independent of the mesh size h , such that

$$\|\mathbf{v}_h\|_{0,\Omega} \leq C_P \|\mathbf{v}_h\|_Z.$$

Thus, by the inf-sup condition for the bilinear form (25a), the discrete adjoint relation (23) and the equation (12a) with staggered continuous test function $\phi_h \in [\mathcal{W}_c^h]^2$, we have

$$\begin{aligned} \|\mathbf{u}_h\|_{0,\Omega} &\leq C_P \|\mathbf{u}_h\|_Z \leq \frac{C_P}{\beta_1} \sup_{\phi_h \in [\mathcal{W}_c^h]^2 \setminus \{0\}} \frac{B_h(\phi_h, \mathbf{u}_h)}{\|\phi_h\|_{X'}} \\ &= \frac{C_P}{\beta_1} \sup_{\phi_h \in [\mathcal{W}_c^h]^2 \setminus \{0\}} \frac{B_h^*(\mathbf{u}_h, \phi_h)}{\|\phi_h\|_{X'}} \\ &= \frac{C_P}{\beta_1} \sup_{\phi_h \in [\mathcal{W}_c^h]^2 \setminus \{0\}} \frac{(S_h, \phi_h)_{0,\Omega}}{\|\phi_h\|_{X'}}. \end{aligned}$$

Then, applying the Cauchy–Schwarz inequality on $(S_h, \phi_h)_{0,\Omega}$ and the norm equivalence relation (21) in the space \mathcal{W}_c^h yields

$$\begin{aligned} \|\mathbf{u}_h\|_{0,\Omega} &\leq \frac{C_P}{\beta_1} \sup_{\phi_h \in [\mathcal{W}_c^h]^2 \setminus \{0\}} \frac{(S_h, \phi_h)_{0,\Omega}}{\|\phi_h\|_{X'}} \\ &\leq \frac{C_P}{\beta_1} \sup_{\phi_h \in [\mathcal{W}_c^h]^2 \setminus \{0\}} \frac{\|S_h\|_{0,\Omega} \|\phi_h\|_{0,\Omega}}{\|\phi_h\|_{X'}} \\ &\leq \frac{C_P}{\beta_1} \|S_h\|_{0,\Omega}. \end{aligned} \tag{45}$$

Combining (45) with (44), we can derive the second bound (38) as

$$\|S_h\|_{0,\Omega}^2 \leq C_M^{-1} \|\mathbf{f}\|_{0,\Omega} \|\mathbf{u}_h\|_{0,\Omega} \leq \frac{C_P}{C_M \beta_1} \|\mathbf{f}\|_{0,\Omega} \|S_h\|_{0,\Omega}.$$

Thus, the first bound (37) follows immediately from (45)

$$\|\mathbf{u}_h\|_{0,\Omega} \leq \frac{C_P}{\beta_1} \|S_h\|_{0,\Omega} \leq \frac{C_P^2}{C_M \beta_1^2} \|\mathbf{f}\|_{0,\Omega}.$$

The second bound (38) also directly implies the stability estimates of S_h^μ by the Lipschitz continuity condition (4).

Therefore, making use of the equivalent inf-sup condition (35) and $S_h^\mu - p_h \mathbf{I}_2 \in \mathcal{W}^h \cap [\mathcal{W}_c^h]^2$, we can derive the last bound (40) of the stability estimates.

$$\begin{aligned} \|S_h^\mu - p_h \mathbf{I}_2\|_{0,\Omega} &\leq \|S_h^\mu - p_h \mathbf{I}_2\|_{X'} \\ &\leq \frac{1}{\beta_1'} \sup_{\mathbf{v}_h \in [\mathcal{U}_c^h]^2 \setminus \{0\}} \frac{B_h(S_h^\mu - p_h \mathbf{I}_2, \mathbf{v}_h)}{\|\mathbf{v}_h\|_Z} \\ &= \frac{1}{\beta_1'} \sup_{\mathbf{v}_h \in [\mathcal{U}_c^h]^2 \setminus \{0\}} \frac{(\mathbf{f}, \mathbf{v}_h)_{0,\Omega}}{\|\mathbf{v}_h\|_Z} \\ &\leq \frac{C_P}{\beta_1'} \|\mathbf{f}\|_{0,\Omega}, \end{aligned}$$

where we have used Eq. (12c) with test function $\mathbf{v}_h \in [\mathcal{U}_c^h]^2$, and the discrete Poincaré–Friedrichs inequality.

After applying the previous stability estimate result (39), we obtain the desired result

$$\begin{aligned} \sqrt{2}\|p_h\|_{0,\Omega} &= \|p_h \mathbf{I}_2\|_{0,\Omega} \leq \|S_h^\mu - p_h \mathbf{I}_2\|_{0,\Omega} + \|S_h^\mu\|_{0,\Omega} \\ &\leq \frac{C_P}{\beta'_1} \|f\|_{0,\Omega} + \|S_h^\mu\|_{0,\Omega}. \end{aligned}$$

□

After deriving the stability estimates of the numerical scheme (12), the existence and uniqueness of the approximate solution $(\mathbf{u}_h, S_h, S_h^\mu, p_h)$ follows immediately. Then, we show the optimal convergence of the numerical scheme.

Theorem 2 *Let $\mathbf{u} \in [H^{k+1}(\Omega)]^2$, $S \in [H^{k+1}(\Omega)]^{2 \times 2}$, $S^\mu \in [H^{k+1}(\Omega)]^{2 \times 2}$ and $p \in H^{k+1}(\Omega)$ be the exact solutions of the system (2), and $\mathbf{u}_h \in [\mathcal{U}^h]^2$, $S_h \in \mathcal{W}^h$, $S_h^\mu \in \mathcal{W}^h$ and $p_h \in \mathcal{P}^h$ be the approximate solutions of the system (12). Then, we have the following convergence estimates:*

$$\begin{aligned} &\|\mathbf{u} - \mathbf{u}_h\|_{0,\Omega} + \|S - S_h\|_{0,\Omega} + \|S^\mu - S_h^\mu\|_{0,\Omega} + \|p - p_h\|_{0,\Omega} \\ &\leq Ch^{k+1} \left(\|\mathbf{u}\|_{[H^{k+1}(\Omega)]^2} + \|p\|_{H^{k+1}(\Omega)} + \|S\|_{[H^{k+1}(\Omega)]^{2 \times 2}} \right) \end{aligned} \tag{46}$$

where C is a positive constant, independent of the mesh size h .

Proof In the following proof, we will use C to denote a positive generic constant, independent of the mesh size h , may have different values at any two different places. First, we will show the upper bound of the error in the projection of S_h and then extend it to the projection error of S_h^μ . Note, if we take the test functions $\mathbf{v}_h \in [\mathcal{U}_c^h]^2$ in (9), $\phi_h \in \mathcal{W}^h$ in (7) and $q_h \in \mathcal{P}^h$ in (10) such that $\phi_h - q_h \mathbf{I}_2 \in \mathcal{W}^h \cap [\mathcal{W}_c^h]^2$, then the exact solution $(\mathbf{u}, S, S^\mu, p)$ satisfies the system of equations

$$\begin{aligned} (S, \phi_h)_{0,\Omega} - B_h^*(\mathbf{u}, \phi_h) + C_h^*(\mathbf{u}, q_h) &= 0, \\ B_h(S^\mu, \mathbf{v}_h) - C_h(p, \mathbf{v}_h) &= (\mathbf{f}, \mathbf{v}_h)_{0,\Omega}, \end{aligned}$$

where we have used the results of (41) and (42). Next, subtracting this system by the corresponding equations in the discrete formulation system (12) results in

$$\begin{aligned} (S - S_h, \phi_h)_{0,\Omega} - B_h^*(\mathbf{u} - \mathbf{u}_h, \phi_h) + C_h^*(\mathbf{u} - \mathbf{u}_h, q_h) &= 0, \\ B_h(S^\mu - S_h^\mu, \mathbf{v}_h) - C_h(p - p_h, \mathbf{v}_h) &= 0, \end{aligned}$$

for any test functions $\phi_h \in \mathcal{W}^h$, $q_h \in \mathcal{P}^h$ such that $\phi_h - q_h \mathbf{I}_2 \in \mathcal{W}^h \cap [\mathcal{W}_c^h]^2$ and $\mathbf{v}_h \in [\mathcal{U}_c^h]^2$. Due to the properties (29) and (36) of the interpolators \mathcal{I} and \mathcal{J} , so the above system of Galerkin orthogonality relations can be rewritten as

$$\begin{aligned} (S - S_h, \phi_h)_{0,\Omega} - B_h^*(\mathcal{I}\mathbf{u} - \mathbf{u}_h, \phi_h) + C_h^*(\mathcal{I}\mathbf{u} - \mathbf{u}_h, q_h) &= 0, \\ B_h(\mathcal{J}S^\mu - S_h^\mu, \mathbf{v}_h) - C_h(\pi_h p - p_h, \mathbf{v}_h) &= C_h(p - \pi_h p, \mathbf{v}_h), \end{aligned}$$

for any test functions $\phi_h \in \mathcal{W}^h$, $q_h \in \mathcal{P}^h$ such that $\phi_h - q_h \mathbf{I}_2 \in \mathcal{W}^h \cap [\mathcal{W}_c^h]^2$ and $\mathbf{v}_h \in [\mathcal{U}_c^h]^2$. Here, π_h is the standard conforming finite element interpolation operator for the triangulation \mathcal{T} . Then, we take $\mathbf{v}_h = \mathcal{I}\mathbf{u} - \mathbf{u}_h \in [\mathcal{U}_c^h]^2$, $\phi_h = \mathcal{J}S^\mu - S_h^\mu$ and $q_h = \pi_h p - p_h$. From the symmetry preserving property of the interpolation operator \mathcal{J} in Lemma 3, we know $\mathcal{J}S^\mu$ is symmetric with continuous normal component across edges of \mathcal{F}_p . Thus, combining with the results that the numerical stress tensor $S_h^\mu - p_h \mathbf{I}_2$ also has continuous normal component across edges of \mathcal{F}_p and $\pi_h p$ is continuous across edges of \mathcal{F}_p , we have

$\phi_h - q_h \mathbf{I}_2 \in \mathcal{W}^h \cap [\mathcal{W}_c^h]^2$. Then, summing the above two equations and using the discrete adjoint properties (23) and (26) show

$$(S - S_h, \mathcal{J}S^\mu - S_h^\mu)_{0,\Omega} = C_h(p - \pi_h p, \mathcal{I}\mathbf{u} - \mathbf{u}_h). \tag{47}$$

Therefore, the projection error of S follows as

$$\begin{aligned} \|\mathcal{J}S - S_h\|_{0,\Omega}^2 &\leq C_M^{-1} \int_{\Omega} (\mathcal{J}S - S_h) : (\mathcal{J}S^\mu - S_h^\mu) \, dx \\ &\leq C_M^{-1} \left(\int_{\Omega} (\mathcal{J}S - S) : (\mathcal{J}S^\mu - S_h^\mu) \, dx + C_h(p - \pi_h p, \mathcal{I}\mathbf{u} - \mathbf{u}_h) \right) \\ &\leq C_M^{-1} (\|\mathcal{J}S - S\|_{0,\Omega} \|\mathcal{J}S^\mu - S_h^\mu\|_{0,\Omega} + \|p - \pi_h p\|_P \|\mathcal{I}\mathbf{u} - \mathbf{u}_h\|_Z) \\ &\leq C_M^{-1} (C_L \|\mathcal{J}S - S\|_{0,\Omega} \|\mathcal{J}S - S_h\|_{0,\Omega} + \|p - \pi_h p\|_P \|\mathcal{I}\mathbf{u} - \mathbf{u}_h\|_Z), \end{aligned} \tag{48}$$

where we have used the strongly monotone condition (3), Eqs. (47), (27) and the Lipschitz continuity condition (4). Note, we can derive a upper bound for the term $\|\mathcal{I}\mathbf{u} - \mathbf{u}_h\|_Z$ as follows:

$$\begin{aligned} \|\mathcal{I}\mathbf{u} - \mathbf{u}_h\|_Z &\leq \frac{1}{\beta_1} \sup_{\phi_h \in [\mathcal{W}_c^h]^2 \setminus \{0\}} \frac{B_h(\phi_h, \mathcal{I}\mathbf{u} - \mathbf{u}_h)}{\|\phi_h\|_{X'}} \\ &= \frac{1}{\beta_1} \sup_{\phi_h \in [\mathcal{W}_c^h]^2 \setminus \{0\}} \frac{B_h^*(\mathcal{I}\mathbf{u} - \mathbf{u}_h, \phi_h)}{\|\phi_h\|_{X'}} \\ &= \frac{1}{\beta_1} \sup_{\phi_h \in [\mathcal{W}_c^h]^2 \setminus \{0\}} \frac{B_h^*(\mathbf{u} - \mathbf{u}_h, \phi_h)}{\|\phi_h\|_{X'}} \\ &= \frac{1}{\beta_1} \sup_{\phi_h \in [\mathcal{W}_c^h]^2 \setminus \{0\}} \frac{(S - S_h, \phi_h)_{0,\Omega}}{\|\phi_h\|_{X'}} \\ &\leq \frac{1}{\beta_1} \|S - S_h\|_{0,\Omega}, \end{aligned} \tag{49}$$

where the inf-sup condition (25a), the discrete adjoint property (23), the property of the interpolation operator (29) and the Eq. (12a) have been used. Then, there exists some positive constants δ_1, δ_2 such that Eq. (48) becomes

$$\begin{aligned} 2C_M \|\mathcal{J}S - S_h\|_{0,\Omega}^2 &\leq 2C_L \|\mathcal{J}S - S\|_{0,\Omega} \|\mathcal{J}S - S_h\|_{0,\Omega} + 2(k_P \beta_1)^{-1} \|p \\ &\quad - \pi_h p\|_{0,\Omega} \|S - \mathcal{J}S\|_{0,\Omega} \\ &\quad + 2(k_P \beta_1)^{-1} \|p - \pi_h p\|_{0,\Omega} \|\mathcal{J}S - S_h\|_{0,\Omega} \\ &\leq C_L \left(\delta_1^{-1} \|\mathcal{J}S - S\|_{0,\Omega}^2 + \delta_1 \|\mathcal{J}S - S_h\|_{0,\Omega}^2 \right) \\ &\quad + (k_P \beta_1)^{-1} \left(\|p - \pi_h p\|_{0,\Omega}^2 + \|S - \mathcal{J}S\|_{0,\Omega}^2 \right) \\ &\quad + (k_P \beta_1)^{-1} \left(\delta_2^{-1} \|p - \pi_h p\|_{0,\Omega}^2 + \delta_2 \|\mathcal{J}S - S_h\|_{0,\Omega}^2 \right) \\ &= \left(C_L \delta_1^{-1} + (k_P \beta_1)^{-1} \right) \|S - \mathcal{J}S\|_{0,\Omega}^2 \end{aligned}$$

$$\begin{aligned}
 &+ \left((k_P \beta_1)^{-1} + (k_P \beta_1 \delta_2)^{-1} \right) \|p - \pi_h p\|_{0,\Omega}^2 \\
 &+ \left(C_L \delta_1 + (k_P \beta_1)^{-1} \delta_2 \right) \|\mathcal{J}S - S_h\|_{0,\Omega}^2
 \end{aligned}$$

Note, [12] shows the interpolation error result for π_h as $\|p - \pi_h p\|_{0,\Omega} \leq Ch^{k+1}|p|_{H^{k+1}(\Omega)}$. Therefore, choosing δ_1, δ_2 such that $2C_M - C_L \delta_1 - (k_P \beta_1)^{-1} \delta_2 > 0$, and applying the interpolation error for \mathcal{J} and π_h , we have the desired projection error

$$\|\mathcal{J}S - S_h\|_{0,\Omega} \leq Ch^{k+1} \left(\|p\|_{H^{k+1}(\Omega)} + \|S\|_{[H^{k+1}(\Omega)]^{2 \times 2}} \right). \tag{50}$$

Similarly, the error of projection of S^μ can be obtained by using the Lipschitz continuous condition (4):

$$\begin{aligned}
 \|\mathcal{J}S^\mu - S_h^\mu\|_{0,\Omega} &\leq C_L \|\mathcal{J}S - S_h\|_{0,\Omega} \\
 &\leq Ch^{k+1} \left(\|p\|_{H^{k+1}(\Omega)} + \|S\|_{[H^{k+1}(\Omega)]^{2 \times 2}} \right). \tag{51}
 \end{aligned}$$

And the upper bound of $\|\mathcal{I}u - u_h\|_{0,\Omega}$ arises naturally from the discrete Poincaré–Friedrichs inequality and Eq. (49) as

$$\|\mathcal{I}u - u_h\|_{0,\Omega} \leq \frac{C_P}{\beta_1} \|S - S_h\|_{0,\Omega}. \tag{52}$$

For the estimate of the upper bound of $\|\mathcal{J}(p\mathbf{I}_2) - p_h\mathbf{I}_2\|_{0,\Omega}$, we use again that $S_h^\mu - p_h\mathbf{I}_2 \in \mathcal{W}^h \cap [\mathcal{W}_c^h]^2$, then the inf-sup condition (35) implies

$$\begin{aligned}
 \|\mathcal{J}(p\mathbf{I}_2) - p_h\mathbf{I}_2\|_{0,\Omega} &\leq \|(S_h^\mu - p_h\mathbf{I}_2) - \mathcal{J}S^\mu + \mathcal{J}(p\mathbf{I}_2)\|_{0,\Omega} + \|\mathcal{J}S^\mu - S_h^\mu\|_{0,\Omega} \\
 &\leq \frac{1}{\beta'_1} \sup_{\mathbf{v}_h \in [\mathcal{U}_c^h]^2 \setminus \{0\}} \frac{B_h((S_h^\mu - p_h\mathbf{I}_2) - \mathcal{J}S^\mu + \mathcal{J}(p\mathbf{I}_2), \mathbf{v}_h)}{\|\mathbf{v}_h\|_Z} \\
 &\quad + \|\mathcal{J}S^\mu - S_h^\mu\|_{0,\Omega} \\
 &= \frac{1}{\beta'_1} \sup_{\mathbf{v}_h \in [\mathcal{U}_c^h]^2 \setminus \{0\}} \frac{B_h((S_h^\mu - S^\mu), \mathbf{v}_h) - B_h((p_h\mathbf{I}_2 - p\mathbf{I}_2), \mathbf{v}_h)}{\|\mathbf{v}_h\|_Z} \\
 &\quad + \|\mathcal{J}S^\mu - S_h^\mu\|_{0,\Omega} \\
 &= \|\mathcal{J}S^\mu - S_h^\mu\|_{0,\Omega} \tag{53}
 \end{aligned}$$

where the last two steps follows from the property of the interpolation operator (36) and Eq. (12c).

Therefore, combining the above estimates (50)–(53) and the approximation properties of the interpolation operators in (30) and (34) results in the explicit L^2 -norm error estimates as follows:

$$\begin{aligned}
 \|u - u_h\|_{0,\Omega} &\leq \|u - \mathcal{I}u\|_{0,\Omega} + \|\mathcal{I}u - u_h\|_{0,\Omega} \\
 &\leq Ch^{k+1} \left(\|u\|_{[H^{k+1}(\Omega)]^2} + \|p\|_{H^{k+1}(\Omega)} + \|S\|_{[H^{k+1}(\Omega)]^{2 \times 2}} \right) \\
 \|S - S_h\|_{0,\Omega} &\leq \|S - \mathcal{J}S\|_{0,\Omega} + \|\mathcal{J}S - S_h\|_{0,\Omega} \\
 &\leq Ch^{k+1} \left(\|p\|_{H^{k+1}(\Omega)} + \|S\|_{[H^{k+1}(\Omega)]^{2 \times 2}} \right)
 \end{aligned}$$

$$\begin{aligned} \|S^\mu - S_h^\mu\|_{0,\Omega} &\leq \|S^\mu - \mathcal{J}S^\mu\|_{0,\Omega} + \|\mathcal{J}S^\mu - S_h^\mu\|_{0,\Omega} \\ &\leq Ch^{k+1} \left(\|p\|_{H^{k+1}(\Omega)} + \|S\|_{[H^{k+1}(\Omega)]^{2 \times 2}} \right) \\ \|p - p_h\|_{0,\Omega} &\leq (\sqrt{2})^{-1} (\|p\mathbf{I}_2 - \mathcal{J}(p\mathbf{I}_2)\|_{0,\Omega} + \|\mathcal{J}(p\mathbf{I}_2) - p_h\mathbf{I}_2\|_{0,\Omega}) \\ &\leq Ch^{k+1} \left(\|p\|_{H^{k+1}(\Omega)} + \|S\|_{[H^{k+1}(\Omega)]^{2 \times 2}} \right) \end{aligned}$$

□

5 Numerical Experiments

We consider the nonlinear Stokes equation whose analytic solution is chosen as the solution of the Kovaszny flow problem with the explicit form

$$\begin{aligned} u_1(x, y) &= 1 - \exp(\lambda x) \cos(2\pi y), \\ u_2(x, y) &= \frac{\lambda}{2\pi} (\exp(\lambda x) \sin(2\pi y)), \\ p(x, y) &= \frac{\exp(2\lambda x)}{2} + \bar{p}, \end{aligned}$$

where $\lambda = -\frac{8\pi^2}{Re + \sqrt{Re^2 + 16\pi^2}}$ with $Re = 1$ as the Reynolds number and \bar{p} is a constant chosen such that the zero average condition for the pressure is satisfied.

In all of our examples, we take the computational domain $\Omega = [0, 1]^2$ and $\partial\Omega_D = \partial\Omega$. An illustration of the mesh triangulation is shown in Fig. 2.

Piecewise linear polynomial (i.e. $k = 1$) is used in all the finite element spaces and \mathbf{f}, \mathbf{g}_D are chosen as in (1). Since we are interested in the varying viscosity function, so we test our method with the following six different viscosity functions:

$$\mu_1(\varepsilon) := 2 + \frac{1}{1 + |\varepsilon|} \qquad \mu_2(\varepsilon) := 1 + \exp(-|\varepsilon|)$$

Fig. 2 Triangulation on $\Omega = [0, 1]^2$ with mesh size 1/4

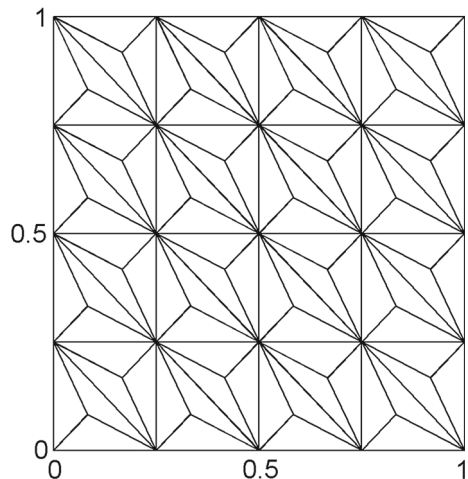


Table 1 The convergence history when $\mu_1(\varepsilon) = 2 + 1/(1 + |\varepsilon|)$

| h^{-1} | $\ u - u_h\ _{0,\Omega}$ | order | $\ S^\mu - S_h^\mu\ _{0,\Omega}$ | order | $\ S - S_h\ _{0,\Omega}$ | order | $\ p - p_h\ _{0,\Omega}$ | order | $\ u - u_h^*\ _{0,\Omega}$ | order | $\ \nabla \cdot u_h^*\ _{L^1(\Omega)}$ | $\ \nabla \cdot u_h^*\ _{L^\infty(\Omega)}$ |
|----------|--------------------------|-------|----------------------------------|-------|--------------------------|-------|--------------------------|-------|----------------------------|-------|--|---|
| 1 | 4.29e-01 | N/A | 8.06e+00 | N/A | 3.82e+00 | N/A | 1.89e+00 | N/A | 2.07e-01 | N/A | 1.53e-06 | 3.83e-07 |
| 2 | 1.88e-01 | 1.19 | 3.54e+00 | 1.19 | 1.68e+00 | 1.18 | 1.22e+00 | 0.64 | 7.83e-02 | 1.40 | 1.48e-14 | 1.10e-14 |
| 4 | 5.42e-02 | 1.79 | 1.14e+00 | 1.64 | 5.36e-01 | 1.65 | 4.91e-01 | 1.31 | 1.62e-02 | 2.27 | 5.39e-14 | 5.27e-14 |
| 8 | 1.42e-02 | 1.93 | 3.48e-01 | 1.71 | 1.63e-01 | 1.72 | 1.58e-01 | 1.64 | 3.19e-03 | 2.35 | 1.83e-13 | 2.45e-13 |
| 16 | 3.57e-03 | 1.99 | 1.01e-01 | 1.78 | 4.75e-02 | 1.78 | 4.71e-02 | 1.74 | 5.91e-04 | 2.43 | 6.71e-13 | 1.05e-12 |
| 32 | 8.88e-04 | 2.01 | 2.82e-02 | 1.85 | 1.32e-02 | 1.84 | 1.33e-02 | 1.83 | 9.67e-05 | 2.61 | 2.69e-12 | 5.44e-12 |
| 64 | 2.21e-04 | 2.01 | 7.52e-03 | 1.91 | 3.53e-03 | 1.91 | 3.57e-03 | 1.90 | 1.40e-05 | 2.79 | 1.09e-11 | 1.92e-11 |

Table 2 The convergence history when $\mu_2(\varepsilon) = 1 + \exp(-|\varepsilon|)$

| h^{-1} | $\ u - u_h\ _{0,\Omega}$ | order | $\ S^\mu - S_h^\mu\ _{0,\Omega}$ | order | $\ S - S_h\ _{0,\Omega}$ | order | $\ p - p_h\ _{0,\Omega}$ | order | $\ u - u_h^*\ _{0,\Omega}$ | order | $\ \nabla \cdot u_h^*\ _{L^1(\Omega)}$ | $\ \nabla \cdot u_h^*\ _{L^\infty(\Omega)}$ |
|----------|--------------------------|-------|----------------------------------|-------|--------------------------|-------|--------------------------|-------|----------------------------|-------|--|---|
| 1 | 4.29e-01 | N/A | 3.81e+00 | N/A | 3.82e+00 | N/A | 9.05e-01 | N/A | 2.04e-01 | N/A | 1.53e-06 | 3.83e-00 |
| 2 | 1.87e-01 | 1.20 | 1.68e+00 | 1.18 | 1.68e+00 | 1.18 | 5.83e-01 | 0.63 | 7.80e-02 | 1.39 | 1.64e-14 | 1.74e-14 |
| 4 | 5.47e-02 | 1.77 | 5.45e-01 | 1.62 | 5.45e-01 | 1.63 | 2.43e-01 | 1.26 | 1.69e-02 | 2.21 | 4.75e-14 | 5.50e-14 |
| 8 | 1.43e-02 | 1.94 | 1.67e-01 | 1.71 | 1.66e-01 | 1.72 | 7.76e-02 | 1.65 | 3.31e-03 | 2.35 | 1.78e-13 | 2.53e-13 |
| 16 | 3.58e-03 | 1.99 | 4.87e-02 | 1.78 | 4.84e-02 | 1.78 | 2.30e-02 | 1.76 | 6.12e-04 | 2.44 | 6.75e-13 | 1.07e-12 |
| 32 | 8.89e-04 | 2.01 | 1.35e-02 | 1.85 | 1.35e-02 | 1.84 | 6.45e-03 | 1.83 | 1.00e-04 | 2.61 | 2.69e-12 | 5.51e-12 |
| 64 | 2.21e-04 | 2.01 | 3.61e-03 | 1.91 | 3.60e-03 | 1.91 | 1.73e-03 | 1.90 | 1.48e-05 | 2.76 | 1.09e-11 | 1.92e-11 |

Table 3 The convergence history when $\mu_3(\varepsilon) = 1 + \exp(-|\varepsilon|^2)$

| h^{-1} | $\ u - u_h\ _{0,\Omega}$ | order | $\ S^\mu - S_h^\mu\ _{0,\Omega}$ | order | $\ S - S_h\ _{0,\Omega}$ | order | $\ p - p_h\ _{0,\Omega}$ | order | $\ u - u_h^*\ _{0,\Omega}$ | order | $\ \nabla \cdot u_h^*\ _{L^1(\Omega)}$ | $\ \nabla \cdot u_h^*\ _{L^\infty(\Omega)}$ |
|----------|--------------------------|-------|----------------------------------|-------|--------------------------|-------|--------------------------|-------|----------------------------|-------|--|---|
| 1 | 4.28e-01 | N/A | 3.82e+00 | N/A | 3.82e+00 | N/A | 9.06e-01 | N/A | 2.03e-01 | N/A | 1.53e-06 | 3.83e-07 |
| 2 | 1.87e-01 | 1.19 | 1.70e+00 | 1.17 | 1.71e+00 | 1.16 | 6.08e-01 | 0.58 | 8.03e-02 | 1.34 | 1.81e-14 | 1.63e-14 |
| 4 | 5.50e-02 | 1.77 | 5.48e-01 | 1.63 | 5.46e-01 | 1.64 | 2.45e-01 | 1.31 | 1.70e-02 | 2.24 | 4.49e-14 | 4.37e-14 |
| 8 | 1.43e-02 | 1.94 | 1.67e-01 | 1.71 | 1.68e-01 | 1.70 | 7.87e-02 | 1.64 | 3.43e-03 | 2.31 | 1.76e-13 | 2.57e-13 |
| 16 | 3.59e-03 | 1.99 | 4.89e-02 | 1.77 | 4.92e-02 | 1.77 | 2.33e-02 | 1.76 | 6.43e-04 | 2.41 | 6.69e-13 | 1.10e-12 |
| 32 | 8.91e-04 | 2.01 | 1.36e-02 | 1.84 | 1.37e-02 | 1.84 | 6.53e-03 | 1.83 | 1.08e-04 | 2.58 | 2.69e-12 | 5.44e-12 |
| 64 | 2.21e-04 | 2.01 | 3.64e-03 | 1.91 | 3.65e-03 | 1.91 | 1.75e-03 | 1.90 | 1.71e-05 | 2.65 | 1.09e-11 | 1.93e-11 |

Table 4 The convergence history when $\mu_4(\varepsilon) = 1/\sqrt{1+|\varepsilon|}$

| h^{-1} | $\ u - u_h\ _{0,\Omega}$ | order | $\ S^\mu - S_h^\mu\ _{0,\Omega}$ | order | $\ S - S_h\ _{0,\Omega}$ | order | $\ p - p_h\ _{0,\Omega}$ | order | $\ u - u_h^*\ _{0,\Omega}$ | order | $\ \nabla \cdot u_h^*\ _{L^1(\Omega)}$ | $\ \nabla \cdot u_h^*\ _{L^\infty(\Omega)}$ |
|----------|--------------------------|-------|----------------------------------|-------|--------------------------|-------|--------------------------|-------|----------------------------|-------|--|---|
| 1 | 4.06e-01 | N/A | 9.73e-01 | N/A | 2.20e+00 | N/A | 3.53e-01 | N/A | 1.60e-01 | N/A | 1.46e-06 | 3.65e-07 |
| 2 | 1.34e-01 | 1.60 | 5.06e-01 | 0.94 | 1.23e+00 | 0.84 | 1.96e-01 | 0.85 | 5.92e-02 | 0.85 | 1.68e-14 | 1.35e-14 |
| 4 | 4.72e-02 | 1.50 | 1.56e-01 | 1.70 | 3.77e-01 | 1.71 | 7.08e-02 | 1.47 | 1.28e-02 | 1.47 | 5.31e-14 | 4.44e-14 |
| 8 | 1.20e-02 | 1.98 | 4.57e-02 | 1.77 | 1.14e-01 | 1.72 | 2.20e-02 | 1.69 | 2.69e-03 | 1.69 | 1.81e-13 | 2.29e-13 |
| 16 | 2.98e-03 | 2.01 | 1.30e-02 | 1.81 | 3.31e-02 | 1.79 | 6.44e-03 | 1.77 | 4.97e-04 | 1.77 | 6.75e-13 | 1.03e-12 |
| 32 | 7.35e-04 | 2.02 | 3.51e-03 | 1.89 | 9.05e-03 | 1.87 | 1.75e-03 | 1.88 | 7.72e-05 | 1.88 | 2.70e-12 | 4.75e-12 |
| 64 | 1.83e-04 | 2.01 | 9.09e-04 | 1.95 | 2.37e-03 | 1.93 | 4.56e-04 | 1.94 | 1.11e-05 | 1.94 | 1.09e-11 | 1.86e-11 |

Table 5 The convergence history when $\mu_5(\varepsilon) = |\varepsilon|$

| h^{-1} | $\ u - u_h\ _{0,\Omega}$ | order | $\ S^\mu - S_h^\mu\ _{0,\Omega}$ | order | $\ S - S_h\ _{0,\Omega}$ | order | $\ p - p_h\ _{0,\Omega}$ | order | $\ u - u_h^*\ _{0,\Omega}$ | order | $\ \nabla \cdot u_h^*\ _{L^1(\Omega)}$ | $\ \nabla \cdot u_h^*\ _{L^\infty(\Omega)}$ |
|----------|--------------------------|-------|----------------------------------|-------|--------------------------|-------|--------------------------|-------|----------------------------|-------|--|---|
| 1 | 4.37e-01 | N/A | 3.16e+01 | N/A | 3.91e+00 | N/A | 4.24e+00 | N/A | 2.28e-01 | N/A | 1.53e-06 | 3.83e-07 |
| 2 | 2.01e-01 | 1.12 | 1.58e+01 | 1.00 | 1.90e+00 | 1.04 | 5.50e+00 | -0.37 | 1.05e-01 | 1.12 | 1.36e-14 | 1.11e-14 |
| 4 | 7.15e-02 | 1.49 | 5.78e+00 | 1.45 | 7.75e-01 | 1.30 | 3.39e+00 | 0.70 | 3.23e-02 | 1.69 | 5.06e-14 | 5.08e-14 |
| 8 | 1.84e-02 | 1.96 | 2.04e+00 | 1.50 | 2.77e-01 | 1.49 | 1.19e+00 | 1.51 | 7.78e-03 | 2.05 | 1.78e-13 | 2.54e-13 |
| 16 | 4.12e-03 | 2.16 | 5.90e-01 | 1.79 | 8.38e-02 | 1.72 | 3.29e-01 | 1.85 | 1.38e-03 | 2.49 | 6.65e-13 | 1.06e-12 |
| 32 | 9.47e-04 | 2.12 | 1.66e-01 | 1.83 | 2.38e-02 | 1.82 | 8.89e-02 | 1.89 | 2.24e-04 | 2.63 | 2.69e-12 | 5.50e-12 |
| 64 | 2.27e-04 | 2.06 | 4.51e-02 | 1.88 | 6.44e-03 | 1.88 | 2.36e-02 | 1.91 | 3.47e-05 | 2.69 | 1.09e-11 | 1.92e-11 |

Table 6 The convergence history when $\mu_6(\varepsilon) = |\varepsilon|^2$

| h^{-1} | $\ u - u_h\ _{0,\Omega}$ | order | $\ S^\mu - S_h^\mu\ _{0,\Omega}$ | order | $\ S - S_h\ _{0,\Omega}$ | order | $\ p - p_h\ _{0,\Omega}$ | order | $\ u - u_h^*\ _{0,\Omega}$ | order | $\ \nabla \cdot u_h^*\ _{L^1(\Omega)}$ | $\ \nabla \cdot u_h^*\ _{L^\infty(\Omega)}$ |
|----------|--------------------------|-------|----------------------------------|-------|--------------------------|-------|--------------------------|-------|----------------------------|-------|--|---|
| 1 | 4.41e-01 | N/A | 2.56e+02 | N/A | 3.95e+00 | N/A | 2.17e+01 | N/A | 2.30e-01 | N/A | 1.53e-06 | 3.83e-07 |
| 2 | 2.13e-01 | 1.05 | 1.37e+02 | 0.90 | 2.07e+00 | 0.93 | 4.15e+01 | 0.93 | 1.18e-01 | 0.96 | 1.79e-14 | 1.60e-14 |
| 4 | 1.01e-01 | 1.08 | 5.77e+01 | 1.24 | 1.07e+00 | 0.95 | 3.40e+01 | 0.29 | 5.28e-02 | 1.16 | 4.67e-14 | 4.55e-14 |
| 8 | 3.80e-02 | 1.41 | 2.63e+01 | 1.13 | 4.85e-01 | 1.15 | 1.62e+01 | 1.07 | 2.10e-02 | 1.33 | 1.80e-13 | 2.61e-13 |
| 16 | 7.43e-03 | 2.35 | 7.66e+00 | 1.78 | 1.47e-01 | 1.72 | 4.74e+00 | 1.78 | 3.89e-03 | 2.43 | 6.67e-13 | 1.08e-12 |
| 32 | 1.34e-03 | 2.47 | 2.07e+00 | 1.89 | 3.99e-02 | 1.88 | 1.23e+00 | 1.94 | 6.01e-04 | 2.69 | 2.69e-12 | 5.54e-12 |
| 64 | 2.94e-04 | 2.19 | 5.58e-01 | 1.89 | 1.07e-02 | 1.90 | 3.21e-01 | 1.94 | 1.14e-04 | 2.40 | 1.09e-11 | 1.93e-11 |

$$\begin{aligned}\mu_3(\varepsilon) &:= 1 + \exp(-|\varepsilon|^2) & \mu_4(\varepsilon) &:= \frac{1}{\sqrt{1 + |\varepsilon|}} \\ \mu_5(\varepsilon) &:= |\varepsilon| & \mu_6(\varepsilon) &:= |\varepsilon|^2,\end{aligned}$$

where $\varepsilon = \varepsilon(\mathbf{u})$ is the strain tensor. The Newton's method is used to solve the resulting system and the Newton iterations stop until the successive error $\|\mathbf{u}_h^{n+1} - \mathbf{u}_h^n\|_{0,\Omega} / \|\mathbf{u}_h^{n+1}\|_{0,\Omega} < 10^{-10}$. We remark that for our simulations, the Newton's method takes approximately 10–20 iterations to achieve the stated stopping condition.

The numerical results show clearly that under different choices of viscosity functions, the L^2 errors of the approximations of the velocity, strain tensor and pressure all converge with an optimal rate $k + 1$. In the last two columns of each table, we measure the L^1 -norm and L^∞ -norm of the divergence of the postprocessed velocity \mathbf{u}_h^* , respectively, and both results show that the numerical solution \mathbf{u}_h^* is exactly divergence free (Tables 1–6).

And we can see that in general, the L^2 errors of the approximations of the postprocessed velocity converges with a superconvergence rate $k + 2$, which also verify our proposition regarding the superconvergence rate of our proposed DG method. However, in Table 6, we can see that the convergence rate of the L^2 errors of the approximations of the postprocessed velocity at the last mesh size level decreases. Possible reasons for this phenomenon include that the rapid increase in the values of $\mu_6(\varepsilon)$ among the domain Ω is difficult to fully capture by our numerical scheme. Another possible reason is that as a posteriori differentiation is required to find the numerical velocity gradient in postprocessing, this process entails a loss of accuracy.

Despite the fact that the convergence rate of \mathbf{u}_h^* is not exactly $k + 2$ for all the examples, we can still see a clear phenomenon that the accuracy is much improved by using an efficient local postprocessing technique. Moreover, the exactly divergence free property of \mathbf{u}_h^* is distinct and is very suitable for applying to fluid flow problems with the incompressibility condition is assumed.

6 Conclusion

In this paper, we developed a discontinuous Galerkin method with a new staggered hybridization technique for the Stokes equation with nonlinear coefficient functions. Our method shares the advantages of the SDG method by the use of staggered hybridization, including mass conservation, optimal convergence and the superconvergence from the local postprocessing technique. Numerical results showed that the postprocessed velocity has better accuracy and is exactly divergence free. Besides, one distinctive feature of our method is the approximate stress tensor is strongly symmetric, so the symmetry of the variable can be best preserved.

Acknowledgements The research of Eric Chung and Xiao-Ping Wang is partially supported by a NSFC/RGC Joint Research Scheme (Project: N_HKUST620/15). The research of Eric Chung is partially supported by Hong Kong RGC General Research Fund (Project number: 14317516).

References

1. Boersma, B.J.: A staggered compact finite difference formulation for the compressible Navier–Stokes equations. *J. Comput. Phys.* **208**(2), 675–690 (2005)
2. Boffi, D., Brezzi, F., Fortin, M., et al.: *Mixed Finite Element Methods and Applications*, vol. 44. Springer, New York (2013)

3. Brenner, S.C.: Poincaré–Friedrichs inequalities for piecewise H^1 functions. *SIAM J. Numer. Anal.* **41**(1), 306–324 (2003)
4. Bustinza, R., Gatica, G.N.: A local discontinuous Galerkin method for nonlinear diffusion problems with mixed boundary conditions. *SIAM J. Sci. Comput.* **26**(1), 152–177 (2004)
5. Cheung, S.W., Chung, E., Kim, H.H., Qian, Y.: Staggered discontinuous Galerkin methods for the incompressible Navier–Stokes equations. *J. Comput. Phys.* **302**, 251–266 (2015)
6. Chung, E., Cockburn, B., Fu, G.: The staggered DG method is the limit of a hybridizable DG method. Part II: The Stokes flow. *J. Sci. Comput.* **66**(2), 870–887 (2016)
7. Chung, E.T., Du, J., Yuen, M.C.: An adaptive SDG method for the Stokes system. *J. Sci. Comput.* **70**, 766–792 (2017)
8. Chung, E.T., Engquist, B.: Optimal discontinuous Galerkin methods for wave propagation. *SIAM J. Numer. Anal.* **44**(5), 2131–2158 (2006)
9. Chung, E.T., Engquist, B.: Optimal discontinuous Galerkin methods for the acoustic wave equation in higher dimensions. *SIAM J. Numer. Anal.* **47**(5), 3820–3848 (2009)
10. Chung, E.T., Lam, M.F., Lam, C. Y.: A staggered discontinuous Galerkin method for a class of nonlinear elliptic equations. *arXiv preprint [arXiv:1610.02331](https://arxiv.org/abs/1610.02331)*, (2016)
11. Chung, E.T., Qiu, W.: Analysis of an SDG method for the incompressible Navier–Stokes equations. *SIAM J. Numer. Anal.* **55**(2), 543–569 (2017)
12. Ciarlet, P.G.: *The Finite Element Method for Elliptic Problems*. SIAM, Philadelphia (2002)
13. Ciarlet, P.G., Glowinski, R., Xu, J.: *Numerical Methods for Non-Newtonian Fluids: Special Volume*, vol. 16. Elsevier, Amsterdam (2010)
14. Cockburn, B., Fu, G., Qiu, W.: A note on the devising of superconvergent hdg methods for Stokes flow by m-decompositions. *IMA J. Numer. Anal.* **37**(2), 730–749 (2017)
15. Cockburn, B., Gopalakrishnan, J.: The derivation of hybridizable discontinuous galerkin methods for stokes flow. *SIAM J. Numer. Anal.* **47**(2), 1092–1125 (2009)
16. Cockburn, B., Gopalakrishnan, J., Lazarov, R.: Unified hybridization of discontinuous Galerkin, mixed, and continuous Galerkin methods for second order elliptic problems. *SIAM J. Numer. Anal.* **47**(2), 1319–1365 (2009)
17. Cockburn, B., Kanschat, G., Schötzau, D., Schwab, C.: Local discontinuous Galerkin methods for the Stokes system. *SIAM J. Numer. Anal.* **40**(1), 319–343 (2002)
18. Girault, V., Rivière, B., Wheeler, M.: A discontinuous Galerkin method with nonoverlapping domain decomposition for the Stokes and Navier–Stokes problems. *Math. Comput.* **74**(249), 53–84 (2005)
19. Grinevich, P.P., Olshanskii, M.A.: An iterative method for the Stokes-type problem with variable viscosity. *SIAM J. Sci. Comput.* **31**(5), 3959–3978 (2009)
20. Isaac, T., Stadler, G., Ghattas, O.: Solution of nonlinear Stokes equations discretized by high-order finite elements on nonconforming and anisotropic meshes, with application to ice sheet dynamics. *SIAM J. Sci. Comput.* **37**(6), B804–B833 (2015)
21. Kim, H.H., Chung, E.T., Lee, C.S.: A staggered discontinuous Galerkin method for the Stokes system. *SIAM J. Numer. Anal.* **51**(6), 3327–3350 (2013)
22. Lee, J.J., Kim, H.H.: Analysis of a staggered discontinuous Galerkin method for linear elasticity. *J. Sci. Comput.* **66**(2), 625–649 (2016)
23. Liu, C., Walkington, N.J.: Convergence of numerical approximations of the incompressible Navier–Stokes equations with variable density and viscosity. *SIAM J. Numer. Anal.* **45**(3), 1287–1304 (2007)
24. Nečas, J.: *Introduction to the Theory of Nonlinear Elliptic Equations*, vol. 52. Teubner, Braunschweig (1983)
25. Nguyen, N., Peraire, J., Cockburn, B.: A hybridizable discontinuous galerkin method for Stokes flow. *Comput. Methods Appl. Mech. Eng.* **199**(9), 582–597 (2010)
26. Qiu, W., Shen, J., Shi, K.: An HDG method for linear elasticity with strong symmetric stresses. *arXiv preprint [arXiv:1312.1407](https://arxiv.org/abs/1312.1407)*, (2013)
27. Qiu, W., Shi, K.: A superconvergent HDG method for the incompressible Navier–Stokes equations on general polyhedral meshes. *IMA J. Numer. Anal.* **36**(4), 1943–1967 (2016)
28. Raviart, P.-A., Girault, V.: *Finite Element Approximation of the Navier–Stokes Equations*. Springer Verlag, New York (1979)
29. Schubert, G., Turcotte, D.L., Olson, P.: *Mantle Convection in the Earth and Planets*. Cambridge University Press, Cambridge (2001)
30. Tavelli, M., Dumbser, M.: A staggered semi-implicit discontinuous Galerkin method for the two dimensional incompressible Navier–Stokes equations. *Appl. Math. Comput.* **248**, 70–92 (2014)